UNITED NATIONS EDUCATIONAL, SCIENTIFIC AND CULTURAL ORGANIZATION
INTERNATIONAL ATOMIC ENERGY AGENCY
INTERNATIONAL CENTRE FOR THEORETICAL PHYSICS
I.C.T.P., P.O. BOX 586, 34100 TRIESTE, ITALY, CABLE: CENTRATOM TRIESTE

H4.SMR/1011 - 2

Fourth Workshop on Non-Linear Dynamics and Earthquake Prediction

6 - 24 October 1997

Application of Block Models to Study of Seismicity

A. SOLOVIEV

International Institute of Earthquake Prediction
Theory and Mathematical Geophysics
Russian Academy of Sciences
Moscow 113 556, Russian Federation

Application of Block Models to Study of Seismicity

A.I.Gorshkov[1,2], G.F.Panza[2,3], I.M.Rotwain[1,2], A.A.Soloviev[1,2], I.A.Vorobieva[1,2]

[1]International Institute of Earthquake Prediction Theory and Mathematical Geophysics Russian Academy of Sciences Moscow, Russia

[2]International Center for Theoretical Physics Trieste, Italy

[3]Dipartimento di Scienze della Terra Universita di Trieste Trieste, Italy

ABSTRACT

The lecture is devoted to application of numerical modelling of block structure dynamics to study of seismicity.

A seismically active region is modelled as a system of absolutely rigid blocks separated by infinitely thin plane faults. The interaction of the blocks along the fault zones and with the underlying medium is viscous-elastic. The system of blocks moves as a consequence of prescribed motion of the boundary blocks and of the underlying medium. When for some part of a fault zone the ratio of the stress to the pressure exceeds a certain strength level, a stress-drop ("failure") occurs (in accordance with the dry friction model), possibly causing failure in other parts of the fault zones. In the model the failures represent earthquakes. As a result of the numerical simulation a synthetic earthquake catalog is produced.

The possibility of earthquakes clustering in the synthetic catalog is considered. The results obtained show that the phenomenon of clustering is observed for a structure consisting of four identical square blocks when a simple movement of one boundary is prescribed.

Numerical modelling was carried out for three groups of structures with increasing structure fragmentation inside each group and for two types of boundary movement. Synthetic earthquake occurrence is characterised by several features, including the frequency-magnitude relation (the Gutenberg-Richter curve). The results obtained show that the features of a synthetic earthquake occurrence obtained by numerical simulation depend on block structure geometry and on the boundary movement. When the structure fragmentation increases, the slope of the Gutenberg-Richter curve changes monotonously in the same direction for all considered groups of structures, provided the boundary movement is the same. The character of the dependence on the geometry is changed dramatically, when the boundary movement of another type is specified.

The procedure is applied to numerical modelling of the dynamics of a block structure, that approximates the tectonic structure of the Vrancea. The result of the numerical experiment is a synthetic earthquake catalog with the spatial distribution of epicenters close to the real distribution and the frequency-magnitude relations obtained for the synthetic and real catalogs possessing some common features.

The dependence of the features of the synthetic earthquake catalog on the prescribed movements of block structure boundaries and of the underlying medium is studied for a model approximating the structure of the Vrancea region and for a model approximating a morphostructural zoning of the Western Alps. The results of the experiments allow us to state that it is possible to use this procedure of block structure dynamics modelling to reconstruct block motions using the observed distribution of epicentres and other seismicity features.

Numerical experiments which illustrate the dependence of the features of a synthetic earthquake catalog on the space model step in the block model were carried out for a structure approximating the main tectonic elements of the Vrancea region and for a structure approximating a morphostructural zoning of the Western Alps.

The studies were partly done in the International Centre for Theoretical Physics (Trieste, Italy) and supported by Russian Foundation for Basic Research (grants RFFI 96-05-65710 and RFFI 97-05-65802), U.S. National Science Foundation (grant EAR 94 23818), and INTAS (grant 94-232).

INTRODUCTION

A seismically active region is modelled as a system of absolutely rigid blocks separated by infinitely thin plane faults. The interaction of the blocks along the fault zones and with the underlying medium is viscous-elastic. The system of blocks moves as a consequence of prescribed motion of the boundary blocks and of the underlying medium. When for some part of a fault zone the ratio of the stress to the pressure exceeds a certain strength level, a stress-drop ("failure") occurs (in accordance with the dry friction model), possibly causing failure in other parts of the fault zones. In the model the failures represent earthquakes. As a result of the numerical simulation a synthetic earthquake catalog is produced. The detailed description of the model is given in Gabrielov and Soloviev (1997) referred below as GS.

The possibility of earthquakes clustering in the synthetic catalog is considered (Gasilov et al., 1995; Maksimov and Soloviev, 1996). It is of vital importance to determine whether clustering is caused by specific tectonic features of a region or is a general phenomenon for a wide variety of neotectonic conditions which reflects general features of systems of interacting blocks of the seismogenic lithosphere. The results obtained show that the phenomenon of clustering is observed for a structure consisting of four identical square blocks when a simple movement of one boundary is prescribed and this clustering of earthquakes in a synthetic catalog arising from modeling of dynamics of a simple block structure is in favour of the second hypothesis. The clustering of earthquakes found in the model allows one to model clustering in specific seismic regions. In particular, the dependence of clustering on block structure geometry and the model parameters can be ascertained.

Numerical modelling was carried out for three groups of structures with increasing structure fragmentation inside each group and for two types of boundary movement (Keilis-Borok et al., 1997). Synthetic earthquake occurrence is characterised by several features, including the frequency-magnitude relation (the Gutenberg-Richter curve). The results obtained show that the features of a synthetic earthquake occurrence obtained by numerical simulation depend on block structure geometry and on the boundary movement. When the structure fragmentation increases, the slope of the Gutenberg-Richter curve changes monotonously in the same direction for all considered groups of structures,

provided the boundary movement is the same. The character of the dependence on the geometry is changed dramatically, when the boundary movement of another type is specified and, what is more, the dependence of seismicity characteristics on structure fragmentation for the boundary movement involving rotation is in contradiction with the views generally had. The structures considered have an artificial geometry and have no exact analogy with the tectonic structure of any real seismic region, in contrast to the structures studied by Gabrielov et al. (1994), Sobolev et al. (1996), and Panza et al. (1997). Nevertheless the dependence of seismicity on tectonic structure fragmentation was detected in certain seismic regions (Hattori, 1974; Kronrod, 1984).

The procedure is applied to numerical modelling of the dynamics of a block structure, that approximates the tectonic structure of the Vrancea region (Panza et al., 1997). The result of the numerical experiment is a synthetic earthquake catalog with the spatial distribution of epicenters close to the real distribution and the frequency-magnitude relations obtained for the synthetic and real catalogs possessing some common features. Therefore it is possible to generate a synthetic catalog that has features similar to those of the real earthquake catalog. The values of the model parameters for which the correspondence between the synthetic and the real catalogs is achieved can be useful for estimating of the velocities of tectonic movements and the values of the physical parameters connected with the dynamic processes taking place in fault zones. If a segment of the synthetic catalog that approximates the real seismicity with sufficient accuracy can be identified, then the part of the synthetic catalog immediately following this segment could be used to predict the future behavior of the seismicity in the region.

The dependence of the features of the synthetic earthquake catalog on the prescribed movements of block structure boundaries and of the underlying medium is studied for a model approximating the structure of the Vrancea region (Vorobieva and Soloviev, 1997). and for a model approximating a morphostructural zoning of the Western Alps (Gorshkov and Soloviev, 1996). The seismic activity of a fault depends on the rate of relative tectonic movements along it, these movements being interrelated in a system of faults. Therefore, the spatial distribution of seismicity can be used not only to compare activity on different faults, but also to reconstruct block motion. It is even possible to formulate the inverse problem: reconstruct block motions using the observed distribution of epicentres and other seismicity features. Such reconstruction becomes possible by using

our model of block structure dynamics. Various numerical experiments carried out by varying the values of model parameters show that the spatial distribution of epicenters is sensitive to the direction of block motion. The results of the experiments allow us to state that it is possible to use this procedure of block structure dynamics modelling to reconstruct block motions using the observed distribution of epicentres and other seismicity features.

Numerical experiments which illustrate the dependence of the features of a synthetic earthquake catalog on the space model step in the block model were carried out for a structure approximating the main tectonic elements of the Vrancea region (V-model) and for a structure approximating a morphostructural zoning of the Western Alps (WS-model). The results of these experiments show that the sensitivity of a block model to space discretization interval ε depends on block structure geometry and the prescribed movements. It follows from them that a synthetic earthquake catalog for which the linear part of the frequency-magnitude plot spans as much as 3 magnitude units can be obtained in a block model. The maximum magnitude and the number of large earthquakes for the WS-model does not change as ε decreases. Therefore for this structure, large earthquakes are not broken up into smaller ones when the space model step decreases. The maximum magnitude and the number of large earthquakes for the V-model decrease (but not dramatically) as the space model step decreases.

MODELLING THE DYNAMICS OF ARTIFICIAL ABSTRACT STRUCTURES

Clustering of Earthquakes in the Model

Investigation of earthquakes clustering is of utmost importance for understanding the dynamics of seismicity, especially for earthquake prediction. That is why this phenomenon has been studied by many researchers, for instance, Kagan and Knopoff (1978), Keilis-Borok et al. (1980), Dziewonski and Prozorov (1984), Molchan and Dmitrieva (1991). It is of vital importance to determine whether clustering is caused by specific tectonics features of a region or is a general phenomenon for a wide variety of neotectonic conditions which reflects general features of systems of interacting blocks of the seismogenic lithosphere. The clustering of earthquakes in a synthetic catalog to be described below arising from modeling of dynamics of a simple block structure is in favour of the second hypothesis.

A feasible mechanism of clustering in the model. Let the block structure consist of two blocks separated by a fault zone and the blocks move translationally with a constant relative velocity vector directed along the fault zone. If the axis X is the line of intersection of the fault with the upper plane, then it follows from (3-6, 9) of GS that

$$\begin{aligned} &f_t = f_x = K(\Delta_t - \delta_t), \\ &f_y = f_l = f_n = p_0 = 0, \\ &\frac{d\delta_t}{dt} = W f_t. \end{aligned} \tag{1}$$

Here $\mathbf{f} = (f_x, f_y)$ is the elastic force per unit area acting along the fault zone, which is the same at all points of the plane; Δ_t is the relative displacement of the blocks; δ_t is the inelastic displacement which is the same at all points of the fault zone, and p_0 the reaction force per unit area.

In accordance with the definition of earthquake and creep given above, earthquakes in this structure occur at equal time intervals, each earthquake involving the whole fault zone, because the value of κ as given by (11) of GS exceeds the level B for the whole fault zone at once.

When the movement of blocks is more intricate, then the value of κ exceeds the level B at different times for different parts of the fault zone. As a result, there is a group (cluster) of smaller earthquakes in place of a single large one.

Example of earthquake clustering in the model. The following block structure was simulated. There are four blocks whose common parts with the upper plane are squares with a side of 50 km (Fig.1). The thickness of the layer d is H = 20 km. All fault zones have the same (85°) angle of dip. It is assumed that the boundary consisting of the fault segments numbered 8 and 7 (Fig.1) moves translationally with the components of velocity V_x = 20 cm and V_y = -5 cm and rotates around the coordinate origin at an angular velocity of 10^{-6} radians. Note that, in accordance with (3) of GS, this movement is equivalent to the translational movement with the components V_x = 20 cm and V_y = 0 and the rotation around the point X = 50 km, Y = 0 (the common point of segments 8 and 7 on the upper plane) with the same angular velocity. The other parts of the structure boundary and the underlying medium do not move.

For all faults the parameters in (5, 6) of GS and the levels for κ ((11) of GS) have the same values: K = 1 bars/cm, W = 0.05 cm/bars, W_s = 1 cm/bars, B = 0.1, H_f = 0.085, H_s = 0.07. For all blocks the parameters in (1, 2) of GS have also the same values: K_u = 1 bars/cm, W_u = 0.05 cm/bars.

The value of P in (11) of GS is 2 Kbars. The discretization is defined by the following values: ε = 5 km, Δt = 0.01.

Note that the dynamics of this block structure is different from the case of two blocks described above. It is related on the one hand to the rotation of the boundary and, on the other, to the presence of four blocks in the structure.

The numerical simulation was made with zero initial conditions. The occurrence times of earthquakes (vertical lines) are shown in Figure 2 for individual fault segments and for the whole structure during the time interval of 3 units starting at t = 480.

Earthquakes occur on six fault segments. The segment 9 has one earthquake only for the period under consideration. Clustering of earthquakes appears clearly on fault segments 1, 3, 6, and 7. Segment 8 has the largest number of earthquakes. Here the clustering appears weaker: the groups of earthquakes are diffuse along the time axis. The picture for the whole structure looks similar, but groups of earthquakes can be identified.

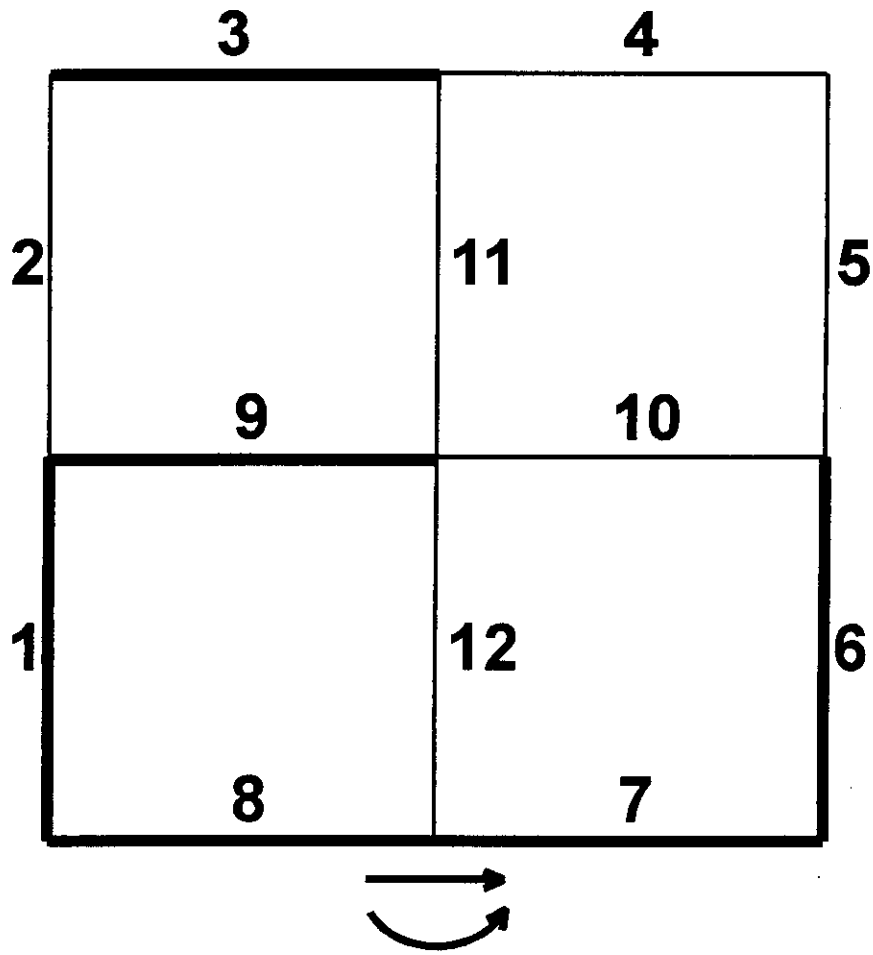

FIGURE 1 The block structure (the numbers of fault segments are indicated) for which clustering is studied.

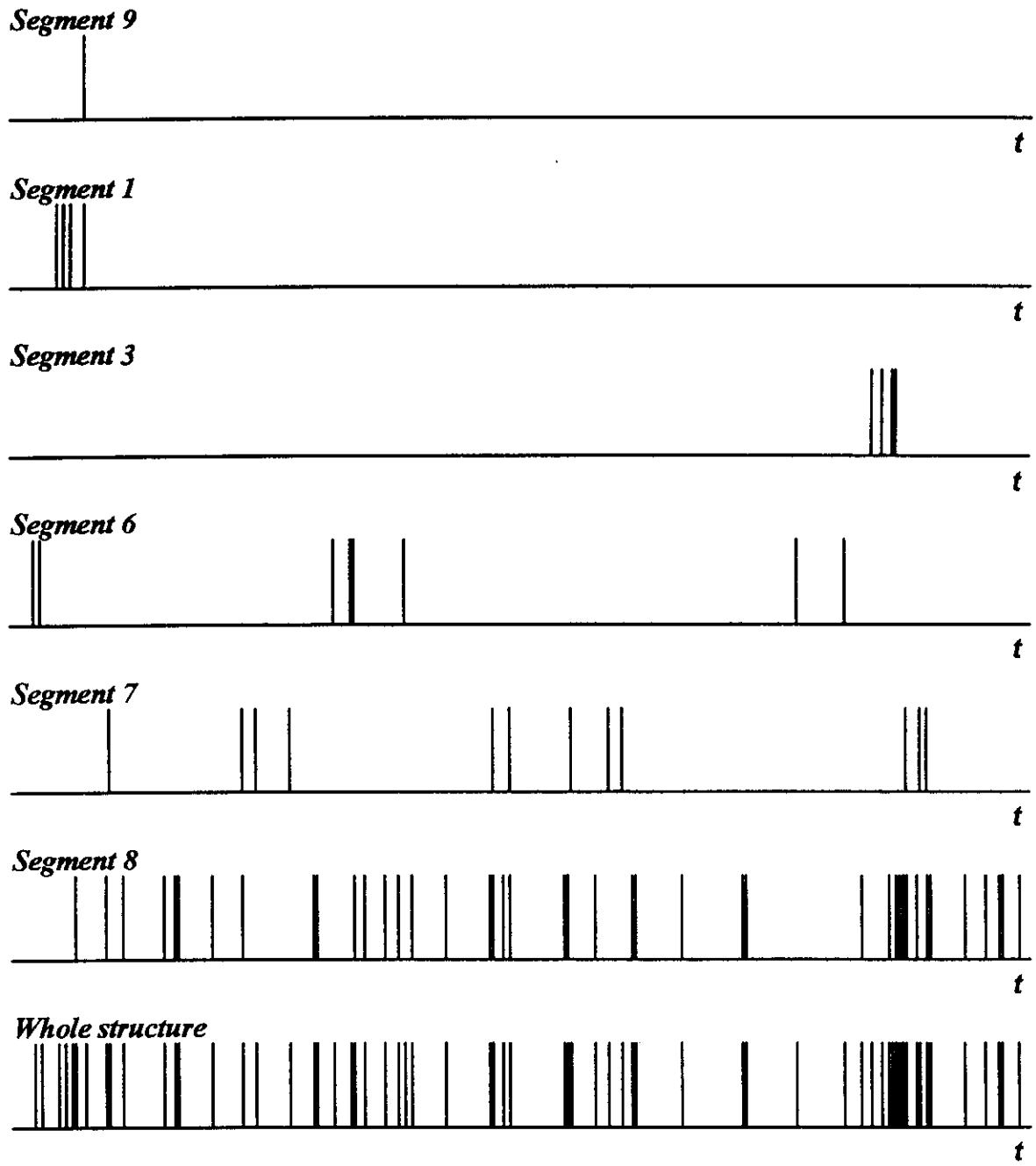

FIGURE 2 Clustering of earthquakes: the times of earthquakes (vertical lines) for individual fault segments and for the whole structure for a time interval of 3 units.

Clustering for other time intervals is not substantially different from that presented in Figure 2.

The clustering of earthquakes found in the model allows one to model clustering in specific seismic regions. In particular, the dependence of clustering on block structure geometry and the model parameters can be ascertained.

Dependence of Synthetic Seismicity on Structure Fragmentation and Boundary Movements

Seismic observations show that features of the seismic process may be different for different regions (see, for example, Hattori, 1974; Kronrod, 1984). It is reasonable to suggest that this difference is due, among other factors, to varying tectonic structure of the regions and main tectonic movements determining the lithosphere dynamics. Laboratory studies show specifically that the differences are largely controlled by the rate of fracturing and heterogeneity of the medium and also by the type of predominant tectonic movements (Mogi, 1962; Sherman et al., 1983; Shamina et al., 1980).

If a single factor is considered, it is difficult to detect its impact on the features of the seismic process by using real seismic observations, because earthquakes are affected by a number of factors some of which could be stronger than the one under consideration. This can be overcome by numerically modelling the earthquake-generating process and studying the synthetic earthquake catalog obtained (see, for example, Allegre et al., 1995; Newman et al., 1995; Shaw et al., 1992; Turcotte, 1992).

Block models in lithosphere dynamics (Gabrielov et al., 1990, 1994; Soloviev, 1995; Panza et al., 1997) are a suitable tool to study the dependence of seismicity features on block structure geometry and movements. Such models can be used to study different types of block structure and of the movements that produce the structure dynamics.

The block model is here used to simulate seismicity for three groups of structures with increasing structure fragmentation within each group and for two types of boundary movements. The dependence of features of synthetic seismicity on structure fragmentation and boundary movement is considered. The features include intensity (number of events during the same time period) of earthquake occurrence, maximum magnitude, and frequency-magnitude relation (the Gutenberg-Richter curve).

Block structures. Numerical simulation was carried out for three groups of block structures. The faults for these structures on the upper plane are shown in Figure 3. One structure (BS1) belongs to all groups. Its faults on the upper plane form a square with a side of 320 km divided into four smaller squares. Two other structures of the first (BS12, BS13), second (BS22, BS23), and third (BS32, BS33) group are obtained from BS1 by subdivision in the self-similar way (Bariere and Turcotte, 1994).

The thickness of the layer d is $H = 20$ km for all structures.

The values of parameters in (1, 2) of GS for all blocks are $K_u = 1$ bar/cm and $W_u = 0.05$ cm/bars.

The parameters in (4-6, 8, 9) of GS for the faults are the following: a = 85° (dip angle); $K = 1$ bar/cm; $W = 0.05$ cm/bars; $W_s = 10$ cm/bars. The levels of κ ((11) of GS) are the same for all faults: $B = 0.1$; $H_f = 0.085$; $H_s = 0.07$.

The value of P in (11) of GS equals 2 Kbars.

Movement. The medium underlying all blocks of the structures does not move.

Two types of boundary movement are considered (Fig.4).

The one type is a translational movement at a velocity of 10 cm per unit non-dimensional time. The directions of the velocity vectors are shown in Figure 4a. The angle between the velocity vector and the proper side of the square outlining a structure is 10°.

The second type involves a translational movement and a rotation (Fig.4b). Two boundaries move translationally at a velocity of 10 cm per unit non-dimensional time. The velocity vectors are parallel to the respective sides of the square that encloses the structure. The other two boundaries rotate about the centers of the respective sides of the square at an angular velocity of $-0.625\ 10^{-6}$ radians per unit non-dimensional time.

It is to be noted that, in the first case, the distribution of $|\mathbf{f}|$ and p_0 along a fault segment is expected to be more uniform than in the second case.

Results of simulation. Numerical simulation of dynamics for all the block structures under consideration was carried out for a period of 200 non-dimensional time units starting from the initial zero condition (zero displacement of the boundary blocks and the underlying medium and zero inelastic displacements for all cells) with both types of boundary movement.

The parameters for time and space discretization are, respectively: $\Delta t = 0.001$, $\varepsilon = 5$ km.

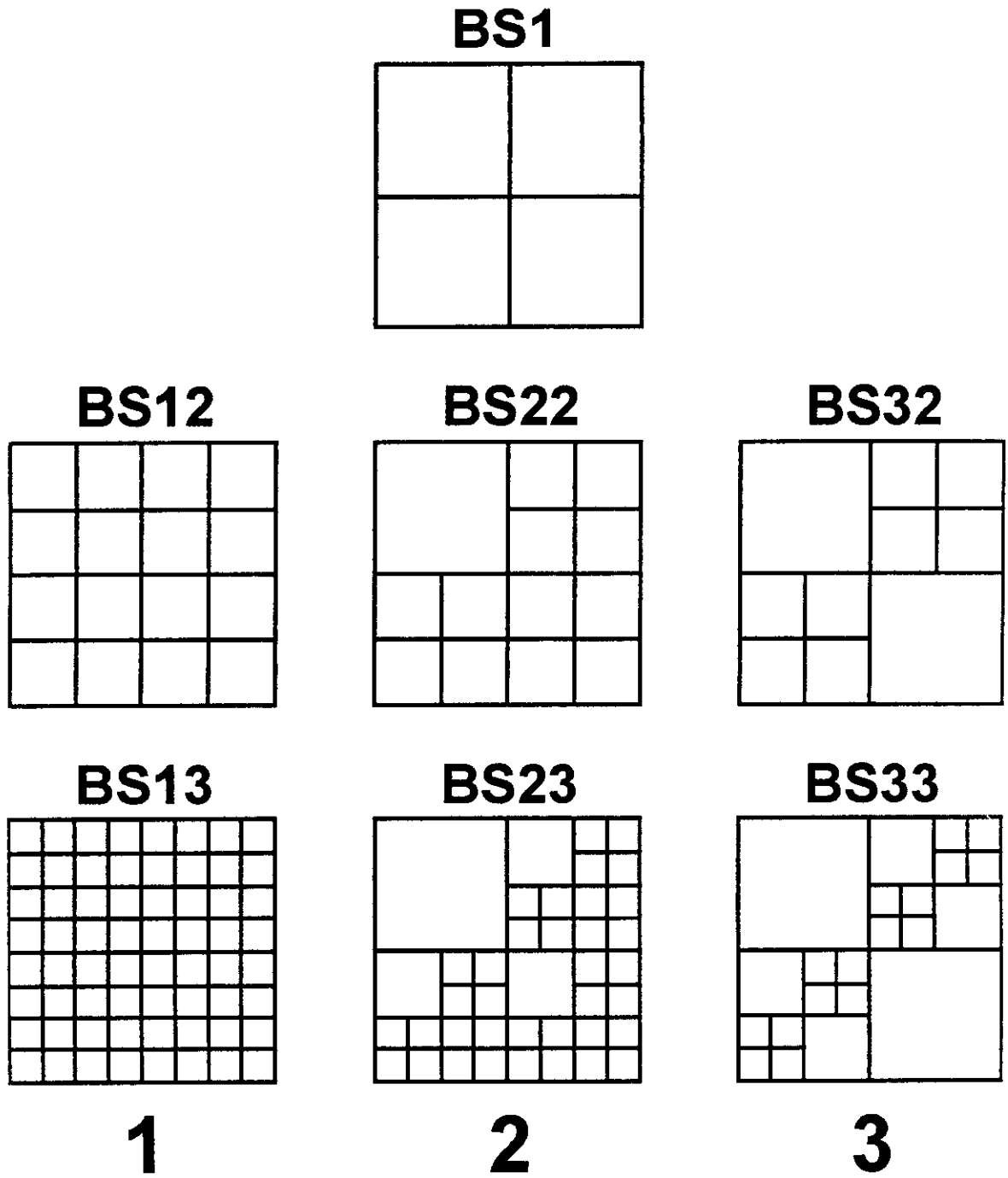

FIGURE 3 Schemes on the upper plane of faults of block structures under consideration: 1 - first group (BS1, BS12, BS13); 2 - second group (BS1, BS22, BS23); 3 - third group (BS1, BS32, BS33).

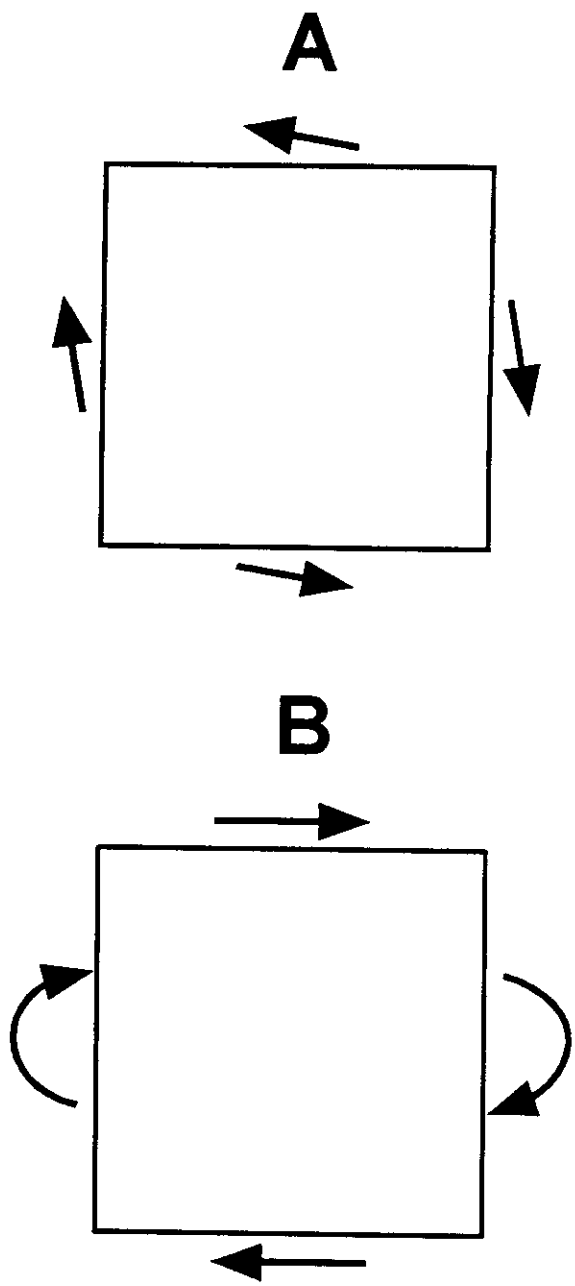

FIGURE 4 Types of the boundary movement considered (the arrows show the vectors of boundaries velocities): *a* - first type, all velocities are 10 cm, the angle between the velocity vectors and the relevant boundary faults is 10°; *b* - second type, the velocities of translational movement is 10 cm, the angular velocity is $-0.625\ 10^{-6}$ radians.

As a result, synthetic earthquake catalogs were obtained. The magnitude of an earthquake was calculated by formula (14) of GS.

It follows from (14) of GS that the lower limit of magnitude for a synthetic catalog is determined by the minimum of cell areas resulting from discretization of the fault segments. In accordance with (14) of GS and the value of ε (5 km), this limit must be less than 5.3. Actually its value depends on the specific structure and varies from 5.12 to 5.18.

The cumulative frequency-magnitude plots for the synthetic catalogs obtained for the first type of boundary movement are presented in Figure 5. The shape of the plots is in accordance with the Gutenberg-Richter law for observed seismicity: the logarithm of the number of earthquakes is a linear function of magnitude.

TABLE 1 Features of seismicity for boundary movement without rotation

Group of structures	Structure	Number of events	Maximum magnitude	*b*-value in magnitude-frequency relation
First	BS1	8801	7.46	.63
	BS12	11417	7.31	.79
	BS13	14163	6.97	1.37
Second	BS1	8801	7.46	.63
	BS22	12692	7.37	.84
	BS23	14670	7.48	1.59
Third	BS1	8801	7.46	.63
	BS32	11986	7.40	.90
	BS33	12366	7.48	1.22

TABLE 2 Features of seismicity for boundary movement with rotation

Group of structures	Structure	Number of events	Maximum magnitude	*b*-value in magnitude-frequency relation
First	BS1	59011	6.20	4.12
	BS12	23748	6.37	3.39
	BS13	5143	6.45	1.9
Second	BS1	59011	6.20	4.12
	BS22	38615	6.31	3.55
	BS23	27110	6.53	2.48
Third	BS1	59011	6.20	4.12
	BS32	53532	6.42	3.59
	BS33	44645	6.61	2.8

Table 1 contains the total number of events (N), maximum magnitude (M_{max}) given by (14) of GS, and estimated slope (b-value) of the frequency-magnitude plot for the catalogs.

The cumulative frequency-magnitude plots for the synthetic catalogs for the second type of boundary movement are presented in Figure 6. Table 2 contains values of N, M_{max}, and b for these catalogs.

Discussion. Figure 5 and Table 1 show that in the case of irrotational boundary movement the cumulative frequency-magnitude plots vary similarly within each group of self-similar structures, when structure fragmentation increases. The following variation is observed: the total number of events and the number of small events increase; the number of large events decreases; the b-value increases. The largest difference between the plots for different structures appears in group 1 (structures BS1, BS12, BS13).

When boundary movement with rotation is considered (Fig.6, Tab.2), the cumulative frequency-magnitude plots also vary similarly in different groups of structures, but when structure fragmentation increases, the variation in each group is ***opposite*** (compared to irrotational boundary movement): the total number of events and the number of small events decrease; the number of large events increases; the b-value decreases. For this type of boundary movement, the largest difference between the plots for different structures is again in the first group.

The larger values of maximum magnitude for irrotational boundary movement (compare Tables 1 and 2) can be explained by the above mentioned fact, namely, that for this type of boundary movement the distribution of $|\mathbf{f}|$ and p_0 along a fault segment is more uniform. Note that in this case earthquakes are mainly caused by large values of $|\mathbf{f}|$ in (11) of GS, whereas in the case of boundary movement with rotation it is the large positive value of p_0 (extension) which plays the main role.

In the case of irrotational (i.e., simpler) boundary movement the change in the b-value with increasing structure fragmentation is largely controlled by the decrease in the number of larger earthquakes. For the boundary movement with rotation (a more complicated case) it is controlled by both the increase in the number of larger earthquakes and, for the first and second groups of structures, by the decrease in the number of smaller events.

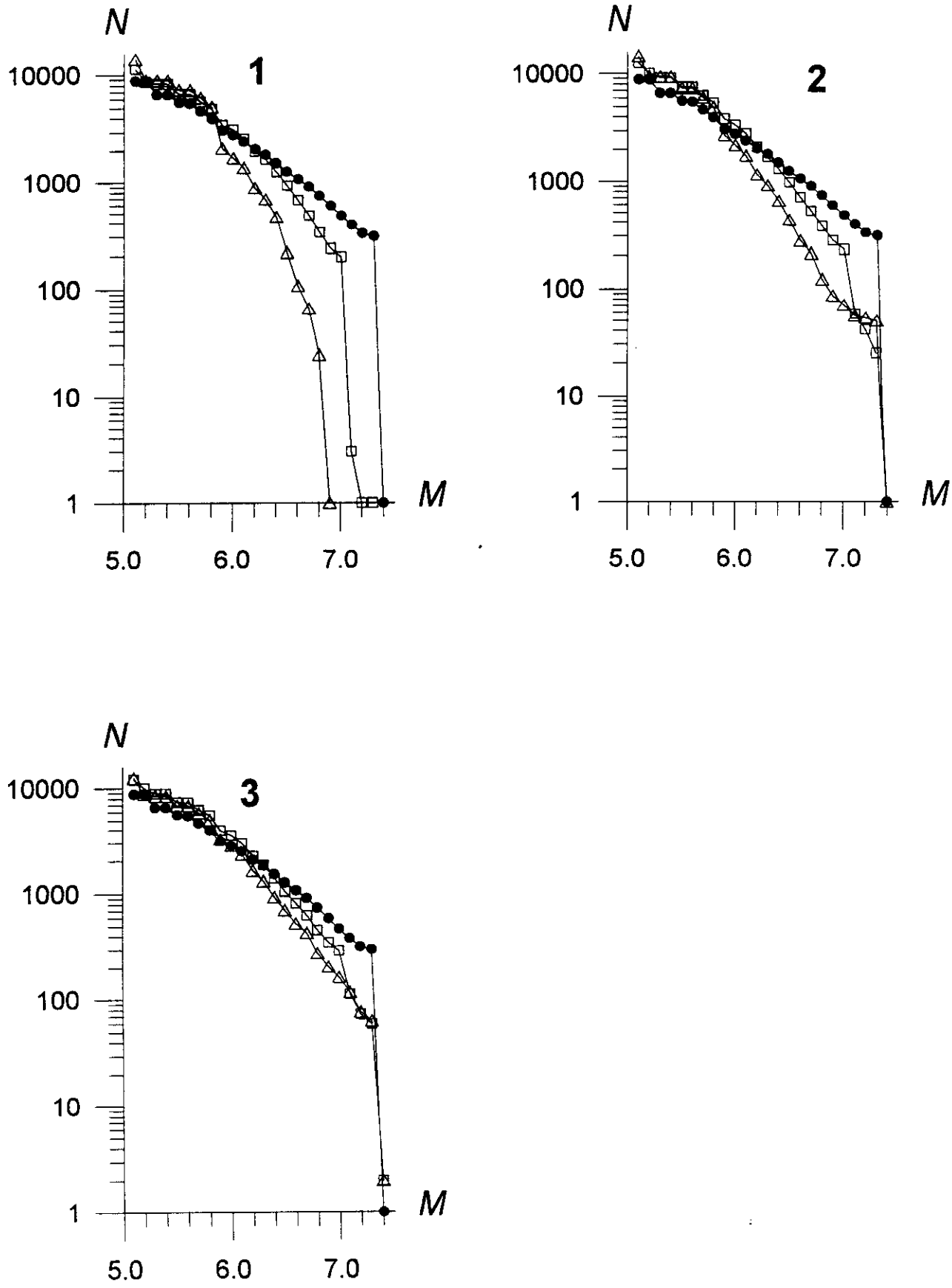

FIGURE 5 Accumulated frequency-magnitude plots (1 - for the first group of the structures, 2 - for the second, 3 - for the third) for the synthetic catalogs obtained with the boundary movement without rotation; dots mark the curves corresponding to BS1, squares - to BS12, BS22, and BS32, triangles - to BS13, BS23, and BS33.

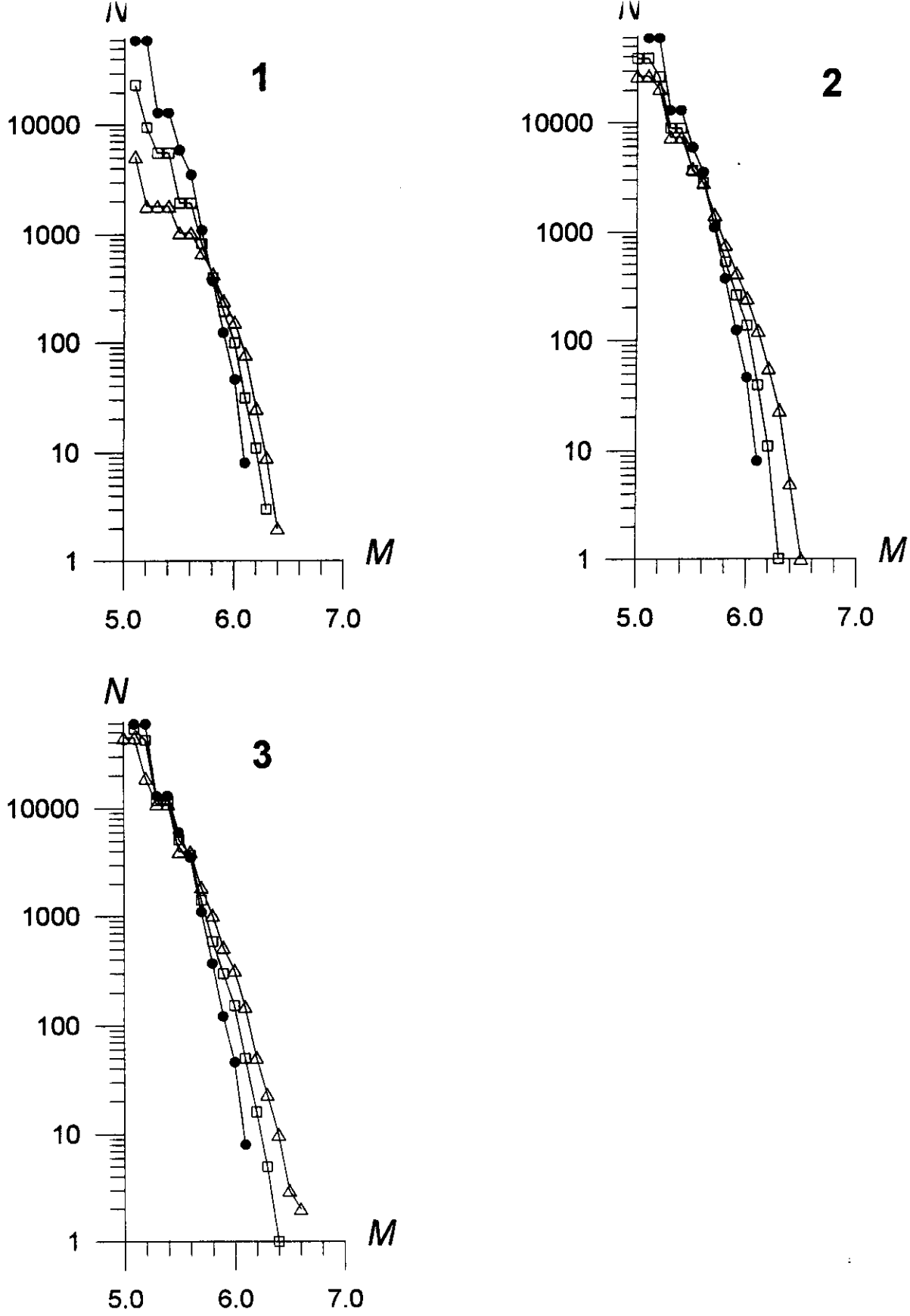

FIGURE 6 Accumulated frequency-magnitude plots for synthetic catalogs obtained with boundary movement with rotation. Notation is the same as in Figure 5.

The results described above show that the features of a catalog obtained by numerical simulation depend on block structure geometry and boundary movement. The character of the dependence on the geometry changes dramatically with the other type of boundary movement. Note that for the boundary movement with rotation the dependence of the above seismicity characteristics on structure fragmentation is in contradiction with the currently accepted view.

The structures considered have an artificial geometry and present no exact analogy with tectonic structure of any real seismic region, in contrast to the structures studied by Gabrielov et al. (1994), Sobolev et al. (1996), and Panza et al. (1997). Nevertheless, the dependence of seismicity features on tectonic structure fragmentation was detected in some seismic regions (Hattori, 1974; Kronrod, 1984). Note that the slope (b-value) of the Gutenberg-Richter curve obtained for irrotational boundary movement (Tab.1, Fig.5) is close to that for the actually observed seismicity (~ 1). For the boundary movement with rotation (Tab.2, Fig.6) the b-value is larger. One is thus confronted with the problem of analysis of seismicity in different seismic regions in order to find similar features in the dependence of seismicity on the fragmentation of tectonic structure.

Relation between the energy and the area. The experience of seismological studies shows that the definition of the magnitude have an essential effect on features of a seismic flow under consideration. The magnitude can be defined on the basis of the earthquake energy (Gutenberg and Richter, 1956)

$$M = 0.67 \lg E - 7.87 \qquad (2)$$

where E is the energy (in ergs) of the earthquake. Formulas (2) and (14) of GS are in accordance with the conventional relation between the energy and the fault surface area

$$E \sim S^{3/2}. \qquad (3)$$

In the model under consideration the sum S of the areas of the cells forming the earthquake is the analogy of the fault surface area. To examine the relation between S and the energy in the model the 2D distributions of events were made for the synthetic catalogs obtained for structure BS32 with the both types of the boundary movement: without rotation (Fig.7a) and with rotation (Fig.7b). Here E is the difference between the energy of the system before and after an earthquake and can be considered as the strain energy released through the earthquake.

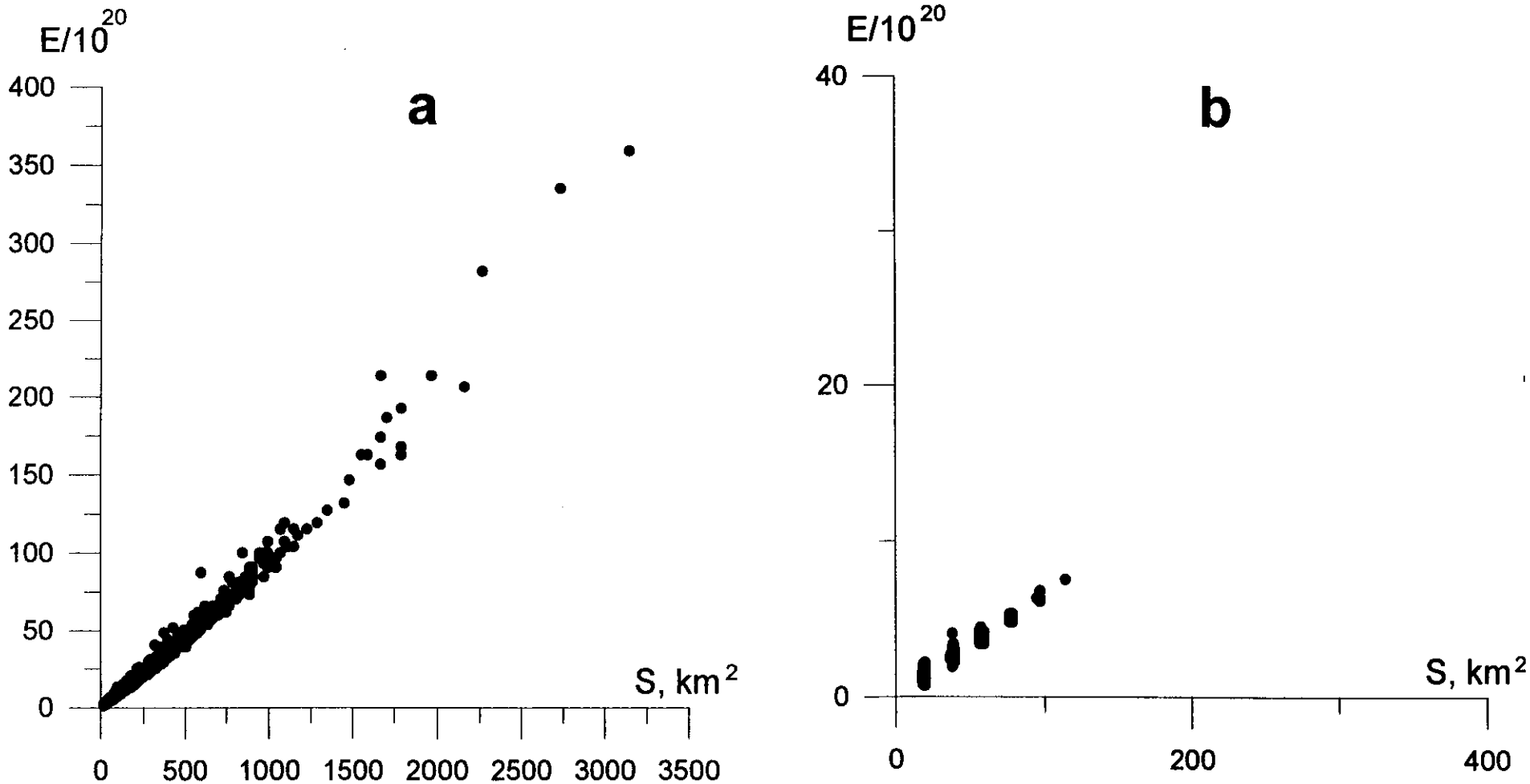

FIGURE 7 Dependence of the energy on the square for the events of the synthetic catalogs obtained for the structure BS32 with the boundary movement without (*a*) and with (*b*) rotation.

It follows from Figure 7 that the relation between the energy, E, released through an earthquake and the total square, S, of the fault plane covered by it is close to the linear law for the both types of the boundary movement. The greatest deviations from this linear law are observed in case of the boundary movement without rotation (Fig.7a) for large earthquakes. These deviations are mainly due to the larger values of E and could be explained by the fact that the average energy release per unit area increases for large earthquakes.

The linear dependence between E and S in the model is in conflict with (3). It causes non-equivalence of formulas (2) and (14) of GS. We explain the linear dependence between E and S by the fact that in the considered model the energy is distributed along planes and the energy released through an earthquake depends mainly on the total square of the fault plane covered by the earthquake. This is an argument to use (14) of GS as a definition of the magnitude in the model at least in case of the same values of constants for all the faults of the block structure.

Note that if formula (2) is used for the definition of the magnitude the plots in figures 5 and 6 endure linear transformation and the properties of the dependence of Gutenberg- Richter curves on structure separateness does not change.

MODELLING THE DYNAMICS OF BLOCK STRUCTURES APPROXIMATING THE TECTONIC STRUCTURE OF REAL SEISMIC REGIONS

Vrancea Region

Structure of the Vrancea region. According to Arinei (1974), the main structural elements of the Vrancea region are: (i) the East-European plate; (ii) the Moesian, (iii) the Black Sea, and (iv) the Intra-Alpine (Pannonian-Carpathian) subplates (Fig.8).

The fault which separates the East-European plate from the Intra-Alpine and Black Sea subplates, and the fault which separates the Intra-Alpine and Black Sea subplates, have the dip angle significantly different from 90° (Mocanu, 1993). The main directions of the relative movement of the plates are shown in Figure 8.

This information is sufficient to define the block structure, which can be considered as a rough approximation to the Vrancea region and to the movements which can be used for numerical simulation.

Block structure used for numerical simulation. The configuration of the faults on the upper plane of the block structure used to model the Vrancea region is presented in Figure 9. The point with the geographic coordinates 44.2°N and 26.1°E is chosen as the origin of the reference system. The X axis is the eastward parallel passing through the origin. The Y axis is the northward meridian passing through the origin.

The thickness of the layer d is H = 200 km, corresponding to the depth of the deeper Vrancea earthquakes.

The vertices with the numbers 1-7 have the following coordinates (in km): (-330; -210), (-270; 480), (450; 90), (110; -270), (0; 270), (-90; 90), (-210; 75).

The vertices 8-11 have the following relative positions on the faults to which they belong: 0.3, 0.33, 0.5, 0.667. The relative position of each vertex is the ratio of its distance from the initial point of the fault to the fault length. The vertices 1, 5, 3, and 10 are considered to be the initial points.

The structure contains 9 faults. The values of the parameters for these faults are given in Table 3, and the values of the parameters for the three blocks are in Table 4.

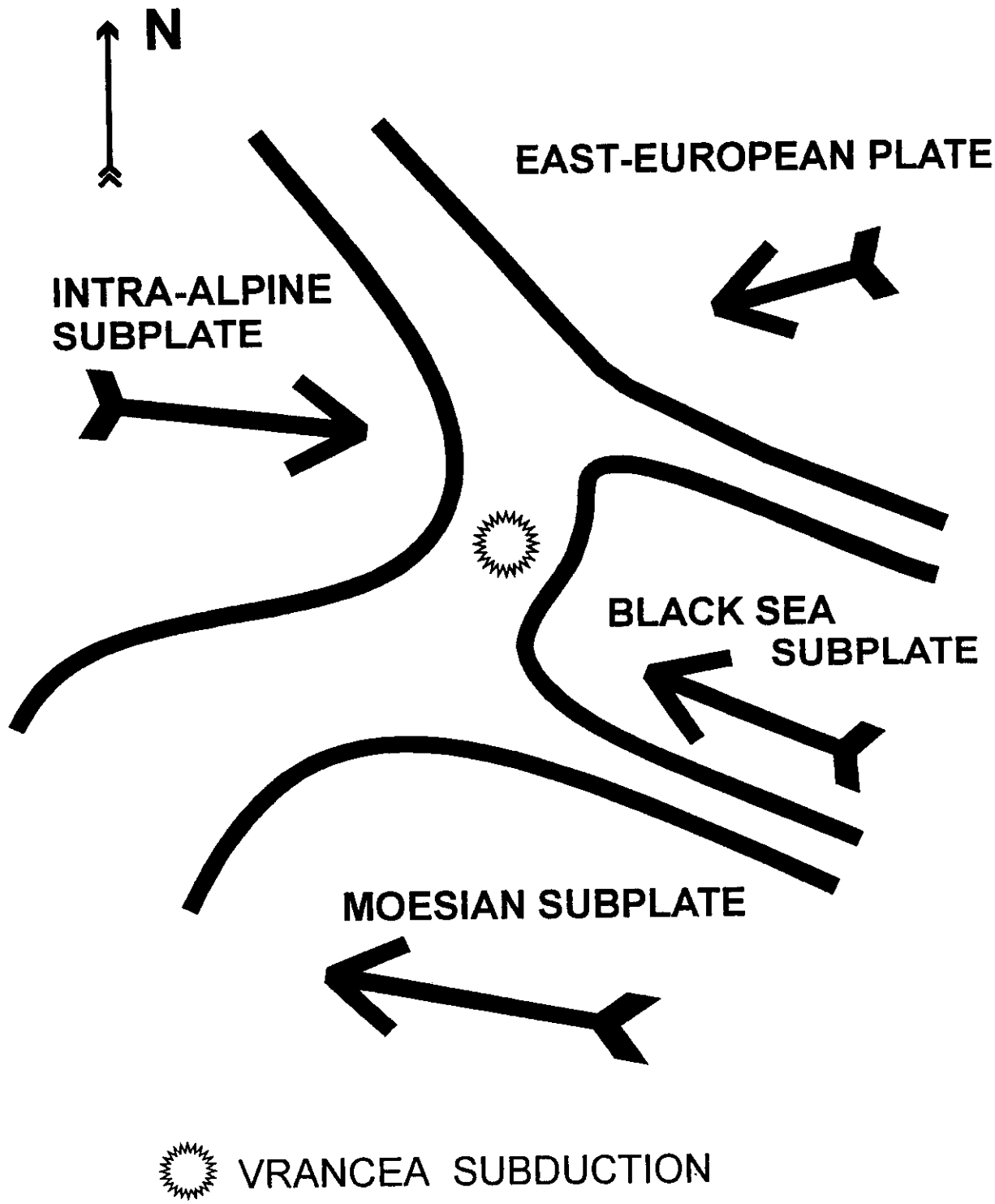

FIGURE 8 Gross kinematic model proposed for the double subduction process in the Vrancea region, modified after Mocanu (1993).

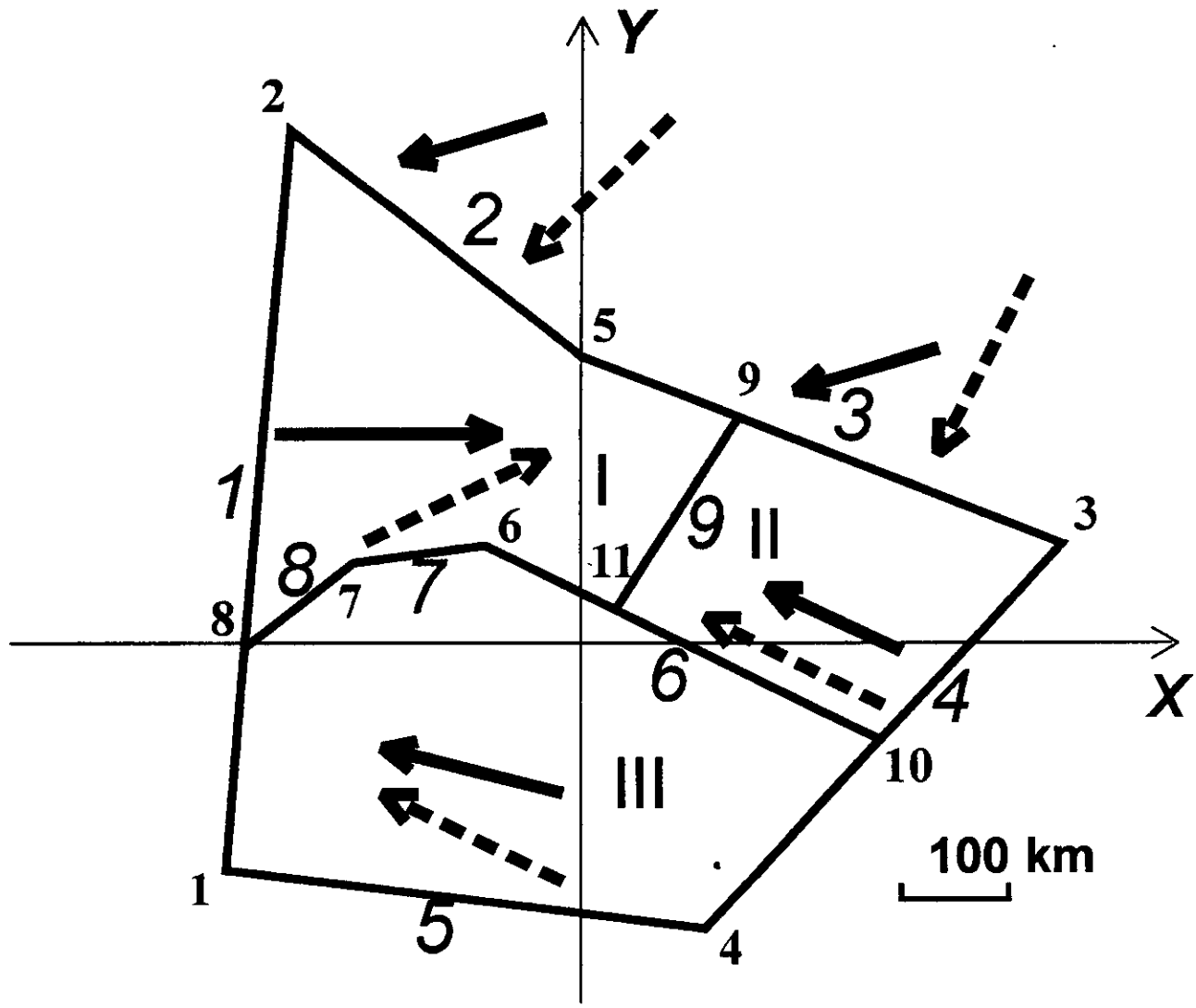

FIGURE 9 The block structure used in numerical simulation; the numbers of vertices (**1 - 11**), faults (*1 - 9*), and blocks (**I - III**) are indicated. The arrows outside the block structure indicate the movement of boundary blocks, while those inside the block structure indicate the movement of the underlying medium. Solid arrows correspond to the map of synthetic epicenters shown in Fig.10, dashed arrows correspond to the map shown in Fig.16.

TABLE 3 Parameters of faults in the Vrancea model

Fault #	Vertices of fault	Dip angle	K, bars/cm	W, cm/bars	W_s, cm/bars	Levels of κ		
						B	H_f	H_s
1	1, 8, 2	45°	0	0	0	0.1	0.085	0.07
2	2, 5	120°	1	0.5	1	0.1	0.085	0.07
3	5, 9, 3	120°	1	0.05	0.1	0.1	0.085	0.07
4	3, 10, 4	45°	0	0	0	0.1	0.085	0.07
5	4, 1	45°	0	0	0	0.1	0.085	0.07
6	10, 11, 6	100°	1	0.05	0.1	0.1	0.085	0.07
7	6, 7	100°	1	0.05	0.1	0.1	0.085	0.07
8	7, 8	100°	1	0.05	0.1	0.1	0.085	0.07
9	11, 9	70°	1	0.02	0.04	0.1	0.085	0.07

TABLE 4 Parameters of blocks in the Vrancea model

Block #	Vertices of block	K_u, bars/cm (see (1))	W_u, cm/bars (see (2))	V_x, cm	V_y, cm
1	2, 8, 7, 6, 11, 9, 5	1	0.05	25	0
2	3, 9, 11, 10	1	0.05	-15	7
3	4, 10, 11, 6, 7, 8, 1	1	0.05	-20	5

The movement of the underlying medium is prescribed to be translational. The velocity components (V_x, V_y) of this movement are prescribed for the blocks in accordance with the directions of the main movements for the Vrancea region shown in Figure 8 and are given in Table 4. Non-dimensional time is used, the values of W and W_s in Table 3, as well as the values of W_u and (V_x, V_y) are given corresponding to the non-dimensional time.

The boundary which consists of faults 2 and 3 moves translationally with the velocity: V_x = -16 cm, V_y = -5 cm. The boundary faults 1, 4, and 5 do not correspond to any real geology of the Vrancea region and are merely introduced to define the block structure completely. Since for these faults K = 0 (Table 3), in accordance with (5) of GS, the relative displacements between the structure blocks and the boundary blocks do not produce the forces in these fault zones.

The value of P in (11) of GS is 2 Kbars.

The magnitude of an earthquake is calculated in accordance with (14) of GS.

The values of the parameters for the time and space discretization are, respectively, Δt = 0.001, ε = 7.5 km.

TABLE 5 Larger Vrancea earthquakes, 1900 - 1995

Date	Time	Hypocenter			Magnitude
		latitude	longitude	depth (km)	
1940/11/10	1.39	45.80°N	26.70°E	133	7.4
1977/03/04	19.21	45.78°N	26.80°E	110	7.2
1986/08/30	21.28	45.51°N	26.47°E	150	7.0
1990/05/30	10.40	45.83°N	26.74°E	110	7.0

Vrancea seismicity. Vrancea is a relatively small seismic region with a high level of seismic activity mainly occurring at intermediate depths. During this century four catastrophic earthquakes with magnitude 7 or greater have occurred (Table 5). An updated Vrancea catalog (Moldoveanu et el., 1995) is used in this work, hence some small discrepancies with Table 1 in Novikova et al. (1995). The Moldoveanu et el. (1995) catalog covers the period 1932 to 1995/03/31, and for the period 1980 to 1993/12/31 it contains only intermediate-depth earthquakes (h > 60 km). Therefore we have supplemented it for the period 1980 -1993 with the shallow events contained in the worldwide NEIC catalog (Global Hypocenters Data Base CD-ROM, 1994). To have a longer period of observation for the Vrancea seismicity we have added to this catalog the one published by Radu (1979), the data for the period before 1932 being from this catalog.

Comparison of synthetic and real catalogs. A synthetic earthquake catalog is obtained as a result of block structure dynamics simulation during a period of 200 non-dimensional time units, starting from the initial zero condition (zero displacement for the boundary blocks and the underlying medium and zero inelastic displacements for all cells).

The synthetic catalog contains 9439 events with magnitudes between 5.0 and 7.6. The minimum value of magnitude corresponds, in accordance with (14) of GS, to the minimum square of one cell. The maximum value of magnitude, 7.6, in the synthetic catalog is close to that actually observed (M = 7.4, see Table 5).

The map showing the epicenters contained in the synthetic catalog is given in Figure 10, while the observed 1900-1995 seismicity is presented in Figure 11.

Most of the synthetic events occurred on fault 9 (cluster A in Figure 10), which corresponds to the Vrancea subduction zone where most observed seismicity is concentrated (cluster A in Figure 11). All large earthquakes (M > 6.7) of the synthetic

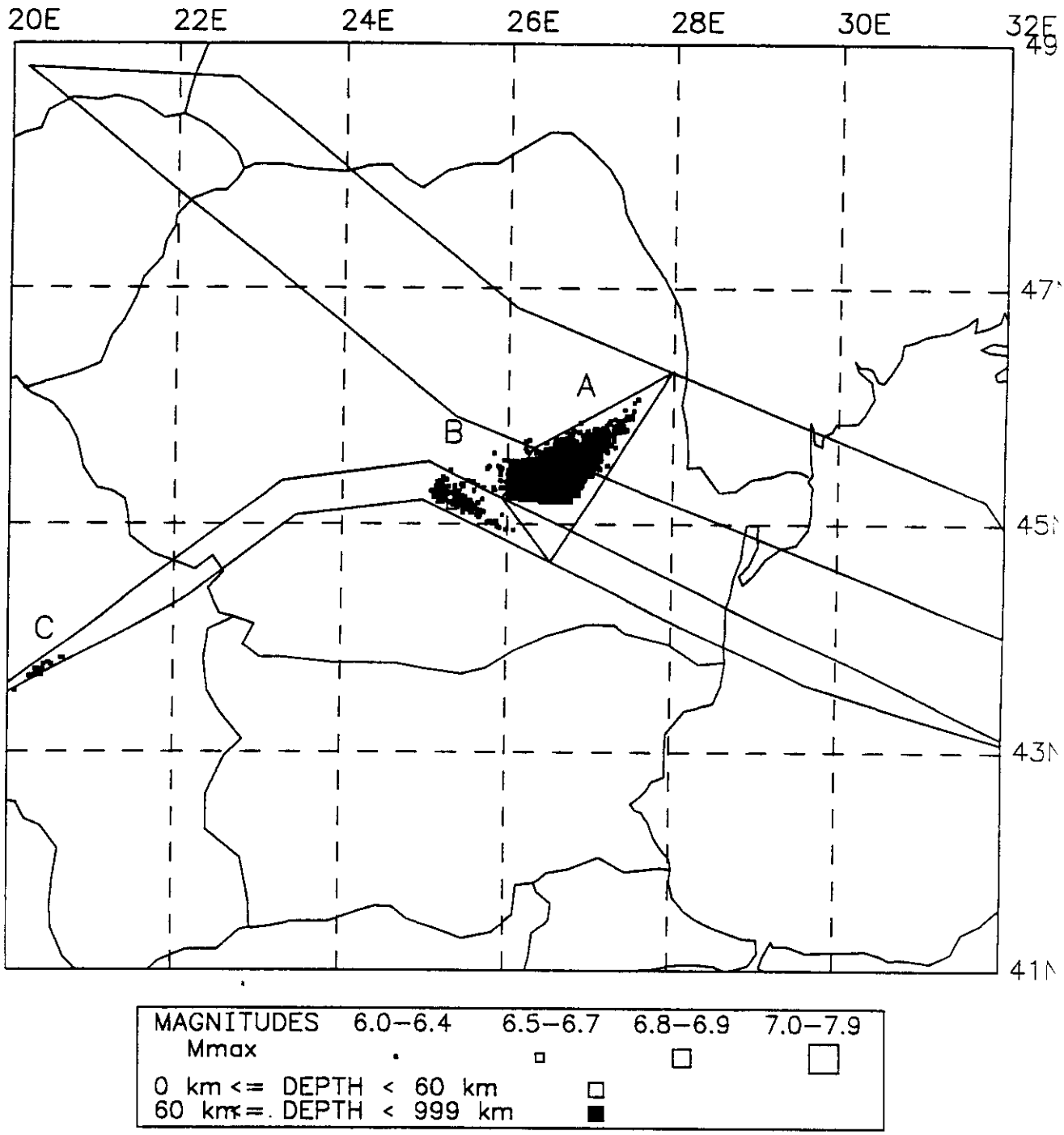

FIGURE 10 Map of simulated seismicity of the Vrancea region, obtained from block structure dynamics. The faults with $K \neq 0$ (solid lines) and the projections on the upper plane of the edges bounding these fault zones and of the lines of intersection between these fault zones and the lower plane (dashed lines) are shown. The movements of blocks and the underlying medium are shown in Fig.9 by solid arrows.

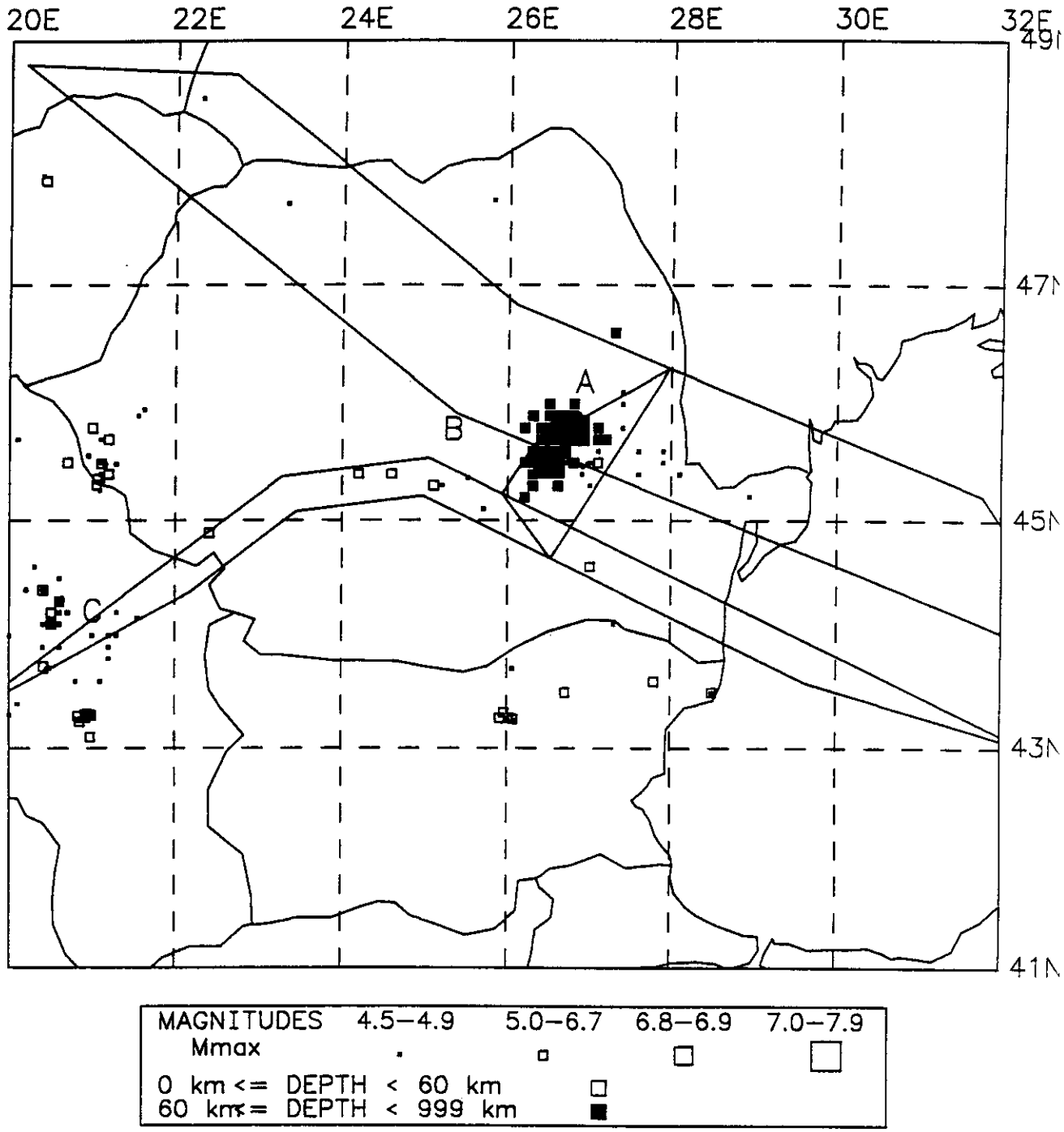

FIGURE 11 Map of observed seismicity in Vrancea for the period 1900-1995. The faults with $K \neq 0$ (solid lines) and the projections on the upper plane of the edges bounding these fault zones and of the lines of intersection between these fault zones and the lower plane (dashed lines) are shown.

catalog are concentrated there, the same phenomenon being seen in the observed seismicity.

Some events occur on fault 6 (marked as cluster *B* in Figure 10) southwest of the bulk of earthquakes and separated from it by an aseismic zone. A similar cluster of epicenters can be seen in the map of observed seismicity (cluster *B* in Figure 11).

The third cluster of events (cluster *C* in Figure 10) is situated on fault 8, corresponding to cluster *C* of observed seismicity in Figure 11.

The map of observed seismicity (Fig.11) contains several more clusters which are absent from the synthetic catalog. This is not surprising, since few main seismogenic faults of the Vrancea region are included in the model. To obtain a more realistic distribution of the synthetic epicenters requires the use of a block structure containing a more detailed description of the real system of faults. Nevertheless the above very simple structure consisting of only three blocks, allows us to reproduce the main features of the spatial distribution of real seismicity.

A time-dependent characteristic of the synthetic catalog is given by the distribution of the number of earthquakes versus magnitude and time as displayed in Table 6. The simulation starts from the initial zero condition, some time being needed for a quasi-stabilization of the stresses. It is possible to estimate the stabilization time using the time-magnitude histogram in Table 6. Starting from 60 units of non-dimensional time, the distribution of the number of events versus magnitude and time looks stable. In the following analysis only the stable part of the synthetic catalog from 60 to 200 non-dimensional time units is considered.

According to the Gutenberg-Richter law for observed seismicity, the logarithm of the number of earthquakes is a linear function of magnitude. The frequency-magnitude plots for observed Vrancea seismicity and for the synthetic catalog are presented in Figure 12. The curve based on the synthetic catalog (dashed line) is almost linear, and has approximately the same slope as that deduced from observed seismicity (solid line).

In the observed seismicity there is a gap in the magnitude interval $6.5 < M < 7.0$ which is not visible in the synthetic catalog. The gap in the observed seismicity may be caused by the small length of the time window for which the observations are available.

TABLE 6 Synthetic catalog: Histogram showing the dependence of the number of events on non-dimensional time, for different magnitude intervals

Time	*Magnitude intervals*														
intervals	5.0-5.2	5.2-5.4	5.4-5.6	5.6-5.8	5.8-6.0	6.0-6.2	6.2-6.4	6.4-6.6	6.6-6.8	6.8-7.0	7.0-7.2	7.2-7.4	7.4-7.6	7.6-7.8	*Total*
0-10	.	.	.	.	.	.	.	.	.	.	.	.	.	.	0
10-20	.	4	15	5	.	.	.	.	.	.	.	.	.	.	24
20-30	.	101	556	148	37	4	.	.	.	.	.	.	.	.	846
30-40	28	102	378	130	60	23	4	.	.	.	.	.	.	.	725
40-50	39	66	247	113	83	47	27	7	1	.	.	.	.	.	630
50-60	6	42	205	76	62	36	24	14	5	1	.	.	.	.	471
60-70	7	51	227	98	67	26	24	11	7	1	2	1	.	.	522
70-80	5	42	207	80	58	40	23	8	8	2	3	.	.	.	476
80-90	8	37	198	87	78	37	20	10	5	.	1	1	.	.	482
90-100	2	41	201	77	70	43	26	9	2	3	3	1	.	.	478
100-110	8	42	181	86	68	35	20	11	6	3	1	.	.	.	461
110-120	9	35	227	81	66	34	17	9	6	2	.	3	.	.	489
120-130	10	37	210	88	56	29	19	9	.	4	2	.	1	.	465
130-140	6	39	204	65	69	33	24	5	4	3	2	2	.	.	456
140-150	7	34	206	80	60	37	15	4	6	2	1	1	.	.	453
150-160	7	49	221	76	67	32	20	7	6	3	1	3	.	.	492
160-170	15	37	227	92	64	23	21	9	5	5	1	1	.	.	500
170-180	12	55	219	62	66	25	19	14	.	1	2	1	.	.	476
180-190	11	42	192	88	68	23	21	7	9	.	.	1	.	1	463
190-200	7	55	220	98	81	31	21	7	7	3	.	.	.	.	530
Total	187	911	4341	1630	1180	558	345	141	77	33	19	15	1	1	9439

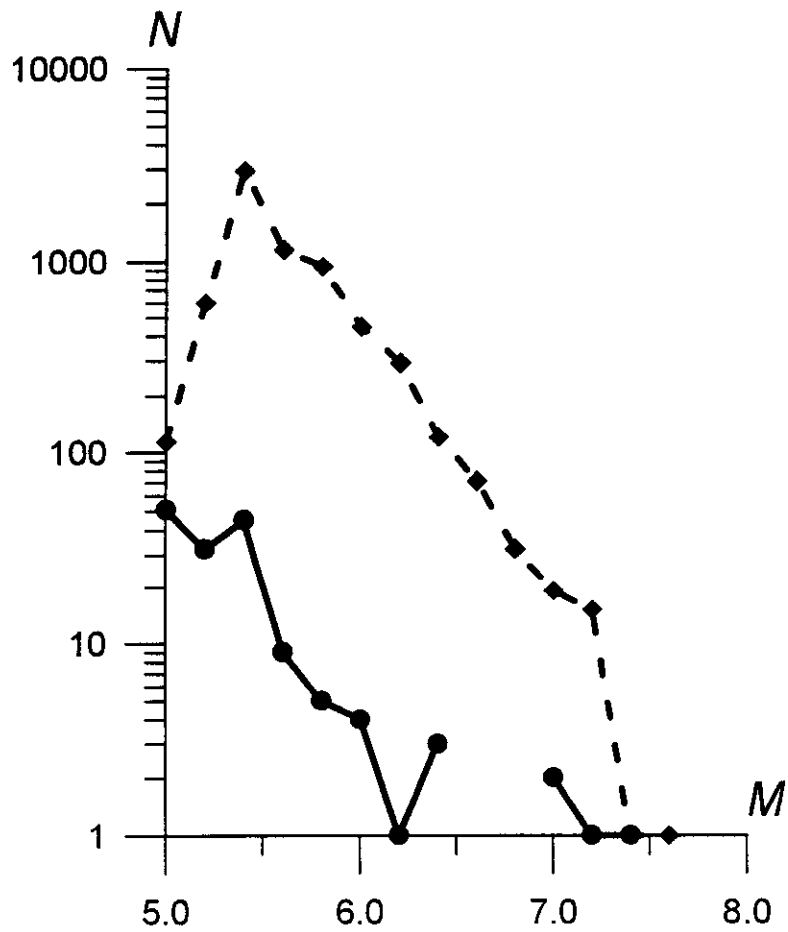

FIGURE 12 Frequency-magnitude plots for the real (solid line) and the synthetic (dashed line) catalogs.

Using the frequency-magnitude plots and the duration of the real catalog (95 years), one can estimate the correspondence of the non-dimensional time with the real one: 140 units of non-dimensional time roughly correspond to 7000 years, or equivalently, 1 unit of non-dimensional time corresponds to about 50 years. From this estimate it follows that the rate of tectonic movements is about 5 mm per year.

The results described above show that, in the Vrancea region, simulation of block structure dynamics generated a synthetic catalog that has features similar to those of the real earthquake catalog.

Instability of the seismic cycle for the synthetic catalog. In accordance with the estimation given above, the duration of the stable part of the synthetic catalog is 70 times larger than that of the real catalog; we therefore divided the synthetic catalog into 70 parts and compared these parts to each other and to the real catalog. The distribution versus magnitude for the 70 parts is presented in Table 7.

The real catalog contains 71 events with $M > 5.4$, the maximum magnitude is 7.4, and there are four large events (Table 5). The number of events with $M > 5.4$ contained in each of the 70 parts of the synthetic catalog varies from 53 to 94, the average number of such events being 68 and the maximum magnitude varying from 6.0 to 7.6 (Table 7). If in the synthetic catalog the events with $M > 6.8$ are considered as large, then the number of large earthquakes varies between 0 and 4. There are no large events in 29 parts, one such event in 20 parts, two in 16 parts, three in 4 parts, and four in 1 part.

Four large events, the same as in the observed contemporary seismicity, occur in a single part of the synthetic catalog. This may indicate that now we live in an "active period" for the Vrancea region.

It is interesting to compare the frequency-magnitude plots for the periods without large earthquakes and for those with several large earthquakes. The slope and level of the frequency-magnitude plots for the real catalog (solid line) and for the synthetic catalog (dashed line) for the period (part 49 in Table 7) without large earthquakes (Fig.13) are quite similar. In the plot for the period (part 16 in Table 7) with four large earthquakes (Fig.14) there is a gap in the magnitude range 6.4-6.8, similar to the observed one. Such a gap is a typical phenomenon for the parts with several large shocks (Table 7).

TABLE 7 Synthetic catalog: The distribution of the number of events versus magnitude for the 70 parts

Part #	*Magnitude intervals*													*Total*	M_{max}
	5.4-5.6	5.6-5.8	5.8-6.0	6.0-6.2	6.2-6.4	6.4-6.6	6.6-6.8	6.8-7.0	7.0-7.2	7.2-7.4	7.4-7.6	7.6-7.8	$M \geq 6.8$		
1	22	18	17	5	5	4	.	.	.	.	.	.	0	71	6.4
2	25	18	9	2	2	2	.	.	.	1	.	.	1	59	7.2
3	26	30	18	9	6	3	1	.	1	.	.	.	1	94	7.1
4	25	12	8	8	5	.	4	.	.	.	.	.	0	62	6.6
5	31	20	15	2	6	2	2	1	1	.	.	.	2	80	7.0
6	24	14	5	10	2	2	3	1	.	.	.	.	1	61	6.8
7	19	20	12	12	6	2	.	.	1	.	.	.	1	72	7.0
8	22	8	13	2	8	2	1	.	1	.	.	.	1	57	7.0
9	25	19	10	8	6	.	3	.	.	.	.	.	0	71	6.6
10	23	19	18	8	1	2	1	1	1	.	.	.	2	74	7.1
11	23	15	14	9	3	3	.	.	.	.	.	.	0	67	6.4
12	21	25	16	2	3	3	1	.	.	.	.	.	0	71	6.6
13	22	19	11	10	4	.	1	.	1	1	.	.	2	69	7.2
14	22	13	24	9	6	1	1	.	.	.	.	.	0	76	6.6
15	20	15	13	7	4	3	2	.	.	.	.	.	0	64	6.6
16	22	15	18	5	9	2	.	1	2	1	.	.	4	75	7.2
17	25	12	15	6	2	2	1	.	.	.	.	.	0	63	6.6
18	23	18	9	10	7	1	1	.	.	.	.	.	0	69	6.6
19	20	19	12	10	5	2	.	2	1	.	.	.	3	71	7.1
20	23	13	16	12	3	2	.	.	.	.	.	.	0	69	6.4
21	21	12	12	10	1	2	1	.	.	.	.	.	0	59	6.6
22	20	24	13	7	5	.	1	2	.	.	.	.	2	72	6.9
23	18	12	9	3	4	1	4	1	1	.	.	.	2	53	7.0
24	22	21	14	7	6	4	.	.	.	.	.	.	0	74	6.4
25	21	17	20	8	4	4	.	.	.	.	.	.	0	74	6.4
26	30	19	14	8	2	3	2	.	.	.	.	.	0	78	6.6
27	30	10	17	5	4	2	2	.	.	2	.	.	2	72	7.3
28	16	15	10	9	4	2	.	1	.	1	.	.	2	58	7.2
29	23	17	14	6	5	1	1	1	.	.	.	.	1	68	6.8
30	30	20	11	6	2	1	1	.	.	.	.	.	0	71	6.6
31	21	19	7	6	2	2	.	1	1	.	.	.	2	59	7.0
32	17	19	8	5	4	2	.	1	.	.	1	.	2	57	7.4
33	19	14	11	4	3	1	.	.	1	.	.	.	1	53	7.0
34	24	15	17	6	7	1	.	1	.	.	.	.	1	71	6.9
35	20	21	13	8	3	3	.	1	.	.	.	.	1	69	6.8
36	23	17	19	6	3	2	2	.	.	.	.	.	0	72	6.6
37	28	17	4	7	7	1	1	.	1	2	.	.	3	68	7.3
38	31	7	18	4	7	1	.	1	.	.	.	.	1	69	6.8
39	17	11	12	8	3	1	1	1	.	.	.	.	1	54	6.9
40	26	13	16	8	4	.	.	1	1	.	.	.	2	69	7.1
41	22	13	12	11	1	1	.	1	1	.	.	.	2	62	7.0
42	18	18	10	8	3	1	1	.	.	1	.	.	1	60	7.3
43	24	15	13	6	2	1	2	1	.	.	.	.	1	64	6.8
44	31	20	11	8	4	.	2	.	.	.	.	.	0	76	6.6
45	22	14	14	4	5	1	1	.	.	.	.	.	0	61	6.6
46	25	17	14	8	1	1	3	1	.	1	.	.	2	71	7.2
47	24	16	17	6	4	2	2	.	1	.	.	.	1	72	7.0
48	25	14	12	6	4	1	.	2	.	1	.	.	3	65	7.2
49	26	19	11	9	2	2	.	.	.	.	.	.	0	69	6.4
50	26	10	13	3	9	1	1	.	.	1	.	.	1	64	7.2
51	20	18	19	6	3	3	.	.	.	.	.	.	0	69	6.4
52	31	20	5	3	2	1	3	1	.	1	.	.	2	67	7.2
53	28	14	9	7	3	1	.	.	.	.	.	.	0	62	6.4
54	27	18	15	4	6	2	.	2	1	.	.	.	3	75	7.0
55	30	22	16	3	7	2	2	2	.	.	.	.	2	84	6.9
56	27	5	11	2	2	5	.	.	2	.	.	.	2	54	7.0
57	26	12	14	9	.	.	.	.	.	.	.	.	0	61	6.0
58	19	17	17	5	6	3	.	.	.	1	.	.	1	68	7.3
59	25	9	12	7	6	3	.	1	.	.	.	.	1	63	6.8
60	25	19	12	2	5	3	.	.	.	.	.	.	0	66	6.4
61	23	22	14	7	4	3	4	.	.	.	.	.	0	77	6.6
62	19	14	11	5	5	2	1	.	.	1	.	1	2	59	7.6
63	19	22	14	3	4	.	.	.	.	.	.	.	0	62	6.2
64	23	16	15	6	5	1	2	.	.	.	.	.	0	68	6.6
65	25	14	14	2	3	1	2	.	.	.	.	.	0	61	6.6
66	24	23	11	5	6	1	2	1	.	.	.	.	1	73	6.8
67	22	20	15	4	1	1	2	1	.	.	.	.	1	66	6.8
68	25	15	16	8	4	2	1	.	.	.	.	.	0	71	6.6
69	23	21	20	8	7	2	1	.	.	.	.	.	0	82	6.6
70	19	16	15	5	2	1	1	1	.	.	.	.	1	60	6.8

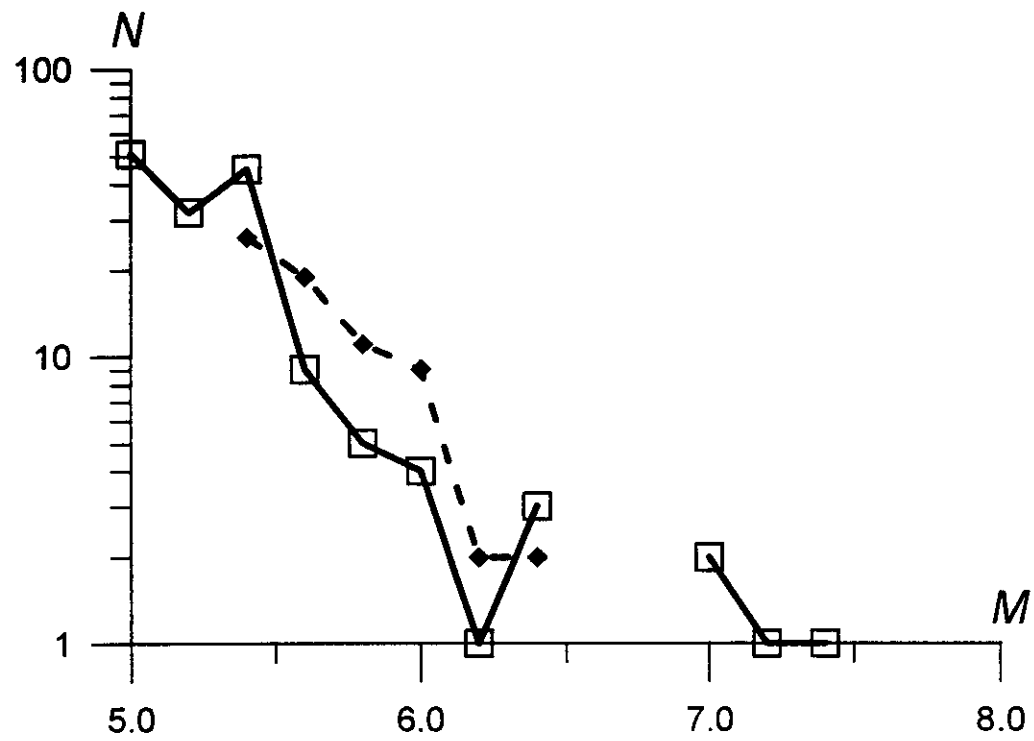

FIGURE 13 Frequency-magnitude plots for the real catalog (solid line) and for part 49 (Table 7) of the synthetic catalog without large earthquakes (dashed line).

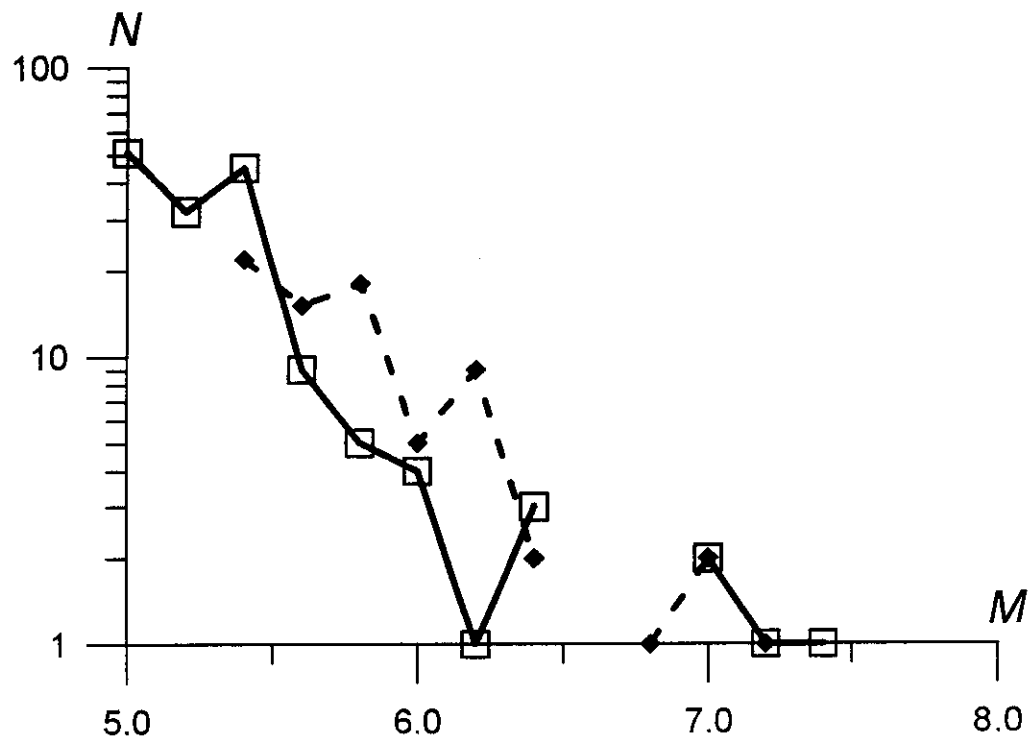

FIGURE 14 Frequency-magnitude plots for the real catalog (solid line) and for part 16 (Table 7) of the synthetic catalog with 4 large earthquakes (dashed line).

The distribution of large ($M > 6.8$) earthquakes in the synthetic catalog for the interval from 60 to 200 units of non-dimensional time (7000 years) presented in Figure 15, shows that the high-magnitude seismicity behaves differently in different time intervals.

For example, in the interval from 70 to 120 units, a periodic occurrence of groups of large earthquakes with a return period of about 6-7 units, corresponding to 300 - 350 years, is observed. The only part (number 16 in Table 7) of the synthetic catalog having four large shocks belongs to this time interval.

For the interval from 120 to 140 units a periodic occurrence of a single large earthquake with a return period of about 2 units, or 100 years, is typical. For the remaining parts of the synthetic catalog one does not notice any periodicity in the occurrence of large earthquakes.

These results show that even the modeled seismic cycle is not stable. Therefore it is necessary to be careful when using the seismic cycle for prediction of a future large earthquake because the available observations cover only a very short time interval compared with the time scale of tectonic processes. This is particularly relevant to the regularity of maxima in the seismic rate for the Vrancea region discussed in Novikova et al. (1995).

The difference found in time behaviour of the simulated earthquake occurrence for different time segments suggests the use of the model for earthquake prediction in the region as follows. If a time segment of the synthetic catalog fitting the real seismicity with sufficient accuracy can be identified, then the part of the synthetic catalog immediately following this segment could be used to predict the future behaviour of the seismicity in the region.

Dependence of synthetic seismicity on prescribed movements of the boundaries and of the underlying medium. The seismic activity of a fault depends on the rate of relative tectonic movements on it, these movements being interrelated in a system of faults. Therefore, the spatial distribution of seismicity can be used not only to compare activity on different faults, but also to reconstruct block motion. It is even possible to formulate the inverse problem: reconstruct block motions using the observed distribution of epicentres and other seismicity features.

Such reconstruction becomes possible by using our model of block structure dynamics. Various numerical experiments carried out by varying the values of the model

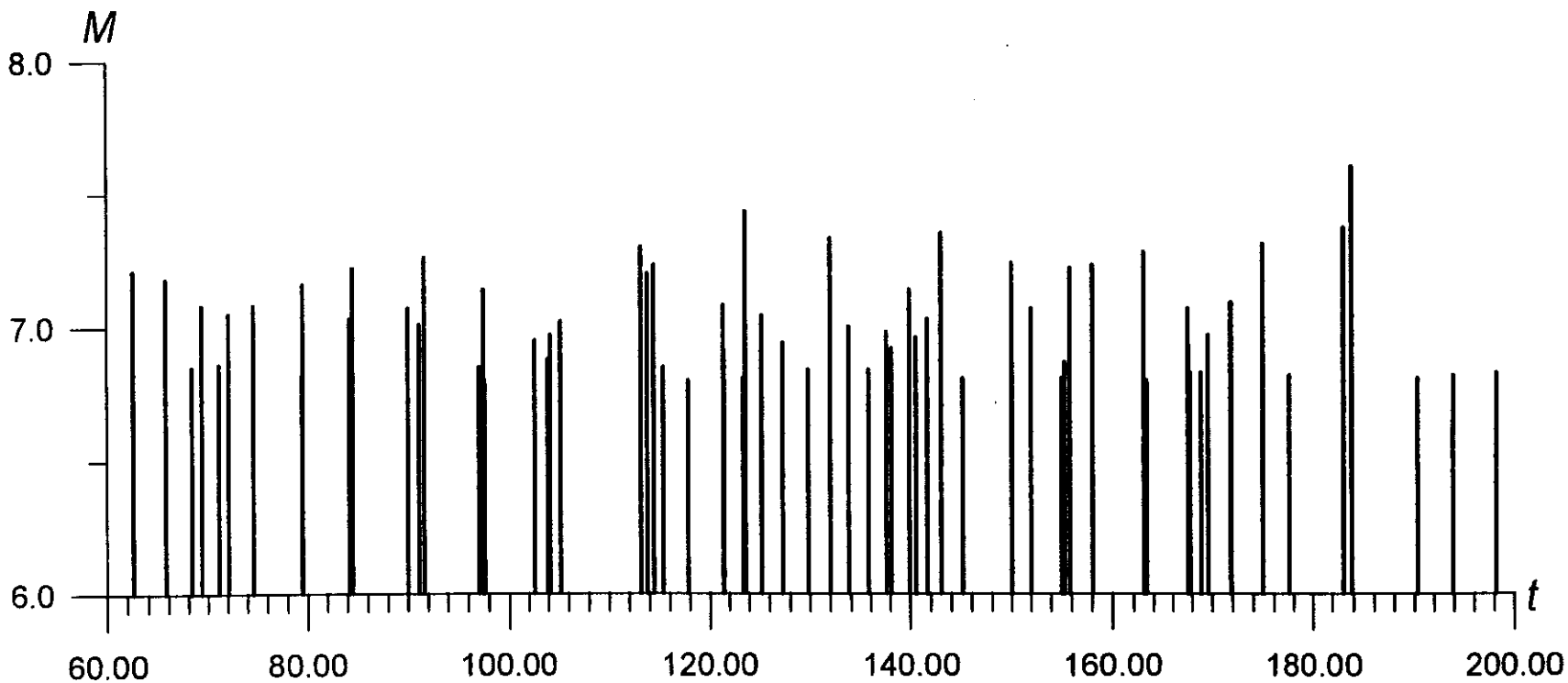

FIGURE 15 Time distribution of large earthquakes in the synthetic catalog for the interval from 60 to 200 units of non-dimensional time (about 7000 years).

parameters show that the spatial distribution of epicenters is sensitive to the direction of block motion.

For example, the distribution of epicenters in the synthetic earthquake catalog obtained for prescribed movements of the boundary and the underlying medium different from those indicated in Figure 9 by solid arrows is shown in Figure 16. The directions of these movements are indicated by dashed arrows in Figure 9. The boundary block adjacent to fault 2 moves translationally with the velocity $V_x = V_y = -16$ cm, while the boundary block adjacent to fault 3 moves translationally with the velocity $V_x = -10$ cm, $V_y = -20$ cm. The underlying medium moves translationally with the following velocities: $V_x = 20$ cm, $V_y = 10$ cm under block 1; $V_x = -20$ cm, $V_y = 10$ cm under blocks 2 and 3.

Comparison of Figures 10 and 16 shows the sensitivity of the space distribution of epicenters to the movements of the boundaries and underlying medium. Note that the directions of the velocities of boundary blocks and of the underlying medium (Fig.9 and Table 4) for which the distribution of epicenters in the synthetic earthquake catalog is similar to the observed one are close to those shown in Figure 8.

The features of the synthetic earthquake catalog depend also on other parameters of the model. Our numerical tests show that the slope of the frequency-magnitude curve increases (a) with decreasing dip angle of fault 9; when the angle exceeds 70°, the seismicity is drastically reduced; (b) with increasing W_s/W, the ratio which determines the rate of growth of inelastic displacements on the fault zones.

The values of the model parameters for which some similarity between the synthetic and the real catalogs is achieved can be useful for estimating the rates of tectonic movements and the physical parameters involved in the dynamic processes in the fault zones.

Western Alps

Block structure. The scheme of morphostructural zoning for the Western Alps (Cisternas et al., 1985) was used as a basis for developing a block structure of that region (Gabrielov et al., 1994; Gasilov et al., 1995). The structure had the same degree of detail as the source map of morphostructural zoning. Low rank lineaments were eliminated from the map to yield a rough morphostructural scheme and a block structure to study the

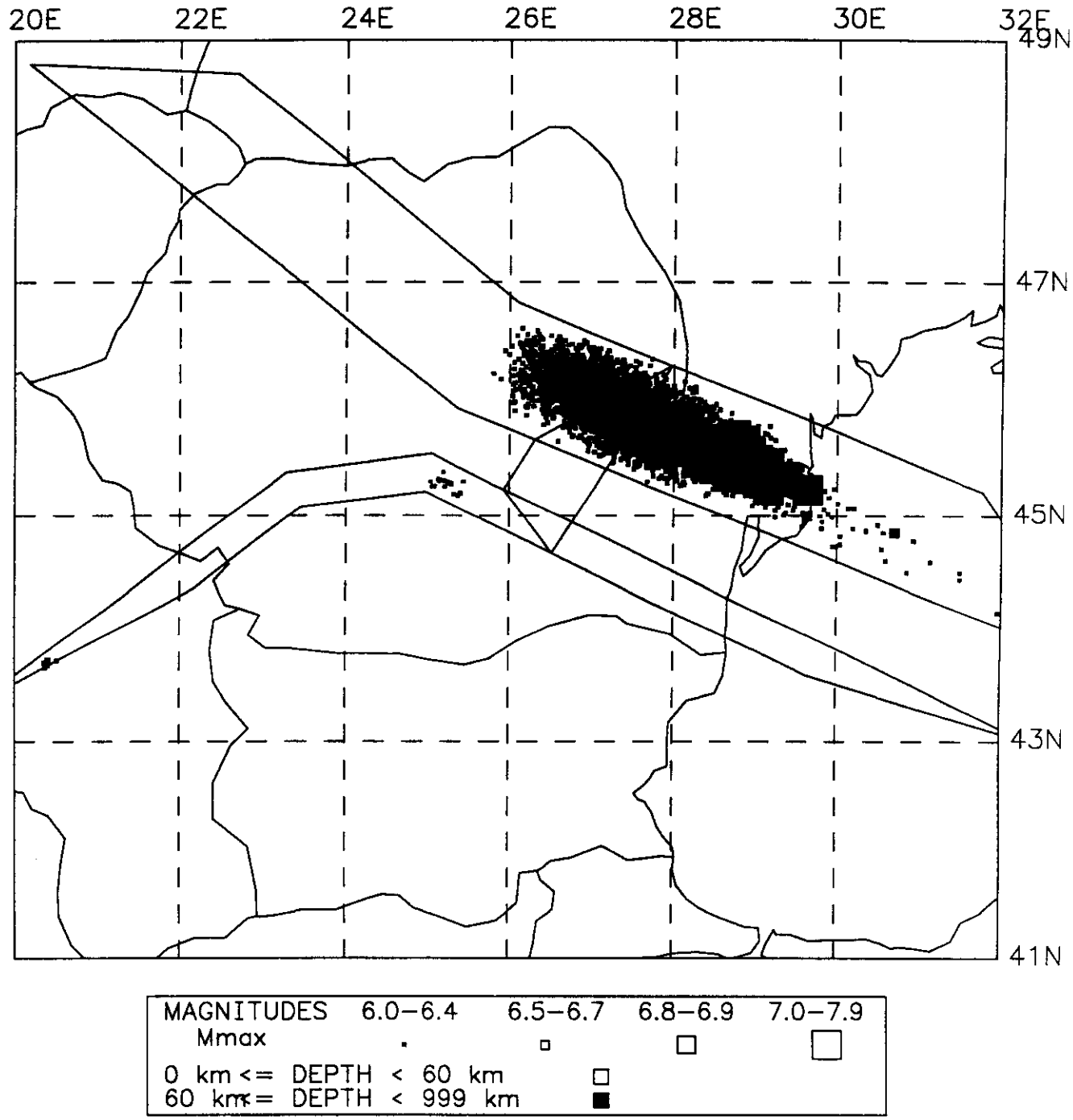

FIGURE 16 Map of synthetic seismicity in the Vrancea region obtained by simulating the block structure dynamics for movements of the boundaries and the underlying medium (dashed arrows in Fig.9) which differ from those for which the map in Figure 10 was obtained.

dependence of simulated seismicity features on boundary movement. The map of morphostructural zoning and the relevant block structure are shown in figures 17 and 18. Note that only high-rank structures, megablocks, were left in the map (Fig.17).

The following values were ascribed to the parameters of the block structure. The thickness of the layer d is H = 30 km. The parameter P in (11) of GS is 2 Kbars. Discretization is defined by the following values: ε = 5 km, Δt = 0.001. The parameters in (5, 6) of GS and the levels for κ ((11) of GS) are the same for all faults: K = 1 bars/cm, W = 0.05 cm/bars, W_s = 10 cm/bars, B = 0.1, H_f = 0.085, H_s = 0.07. The parameters in (1, 2) of GS are also the same for all blocks: K_u = 1 bars/cm, W_u = 0.05 cm/bars. The dip angles of the fault zones are shown in Figure 18.

The Western Alps is a continental collision zone within the Mediterranean orogenic mobile belt. The regional stress field is controlled by the interaction between the Apennine and Western European plates. According to plate tectonics, the Apennine plate moves northwest, causing compression in the Western Alps (McKenzie, 1970). The part of the boundary shown as a double line in Figure 18 (this part corresponds to the boundary between the Alps and the Apennines) moves translationally, while the other parts of the boundary, as well as the underlying medium, do not move. The velocity of boundary movement is 10 cm. The angle between the velocity vector and the north-looking meridian varied between 30° and 90°.

Results. The synthetic earthquake catalogs were obtained as a result of this block structure dynamics simulation, for the period of 200 units of non-dimensional time starting from the initial zero condition (zero displacement of boundary blocks and the underlying medium and zero inelastic displacements for all cells). The accumulated frequency-magnitude plots for the synthetic catalogs are presented in Figure 19.

It follows from Figure 19 that the frequency-magnitude plot depends on the direction of the boundary movement velocity vector. The total number of events in the synthetic catalog decreases when the angle between the velocity vector and the north increases from 30° to 90°: 27210 (30°), 23630 (45°), 19521(60°), 4255 (90°). The shape of the curve for 90° differs significantly from that of the other curves. This curve reflects an abnormal abundance of large earthquakes that can be interpreted as the presence of a "characteristic earthquake".

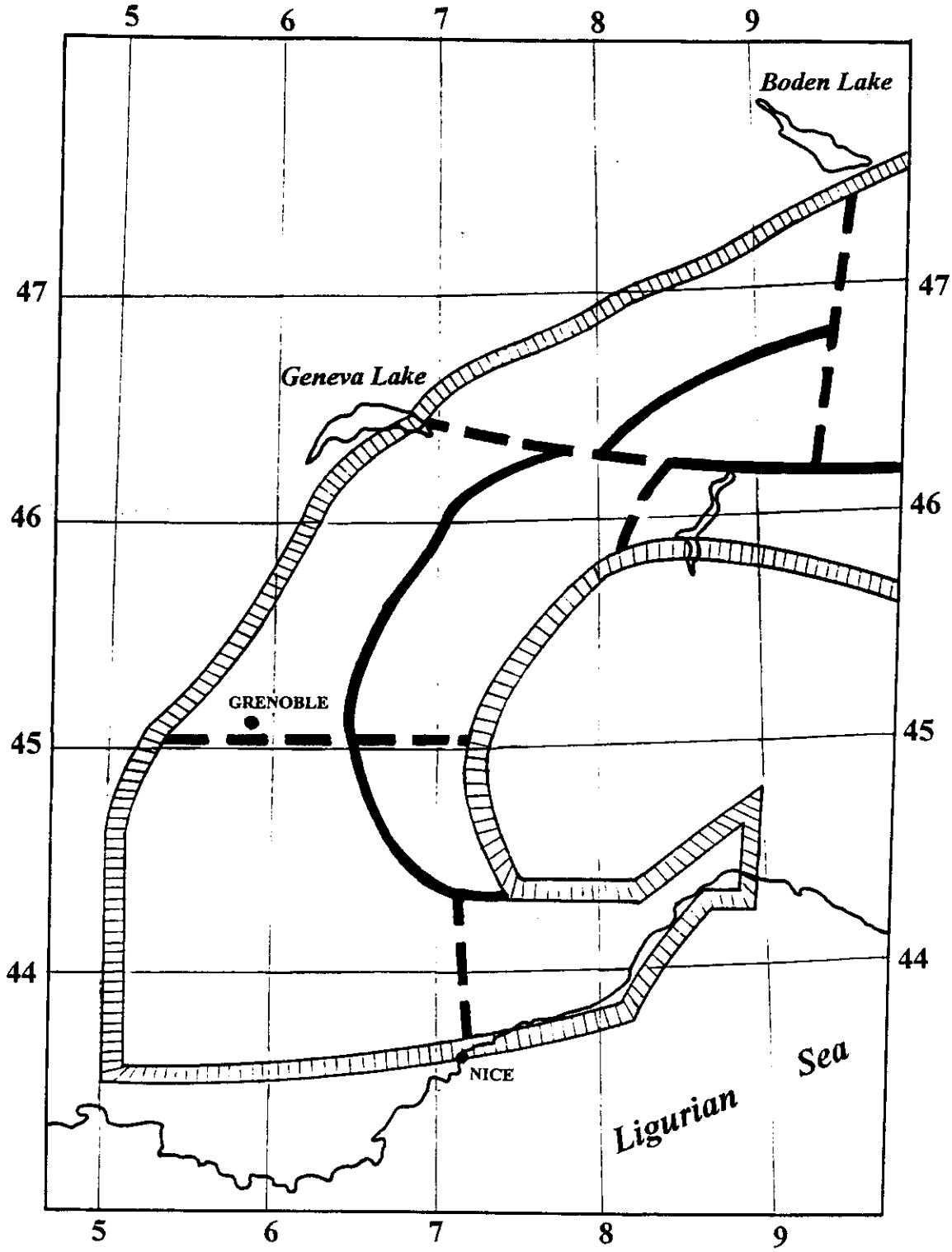

FIGURE 17 Rough map of morphostructural zoning for the Western Alps.

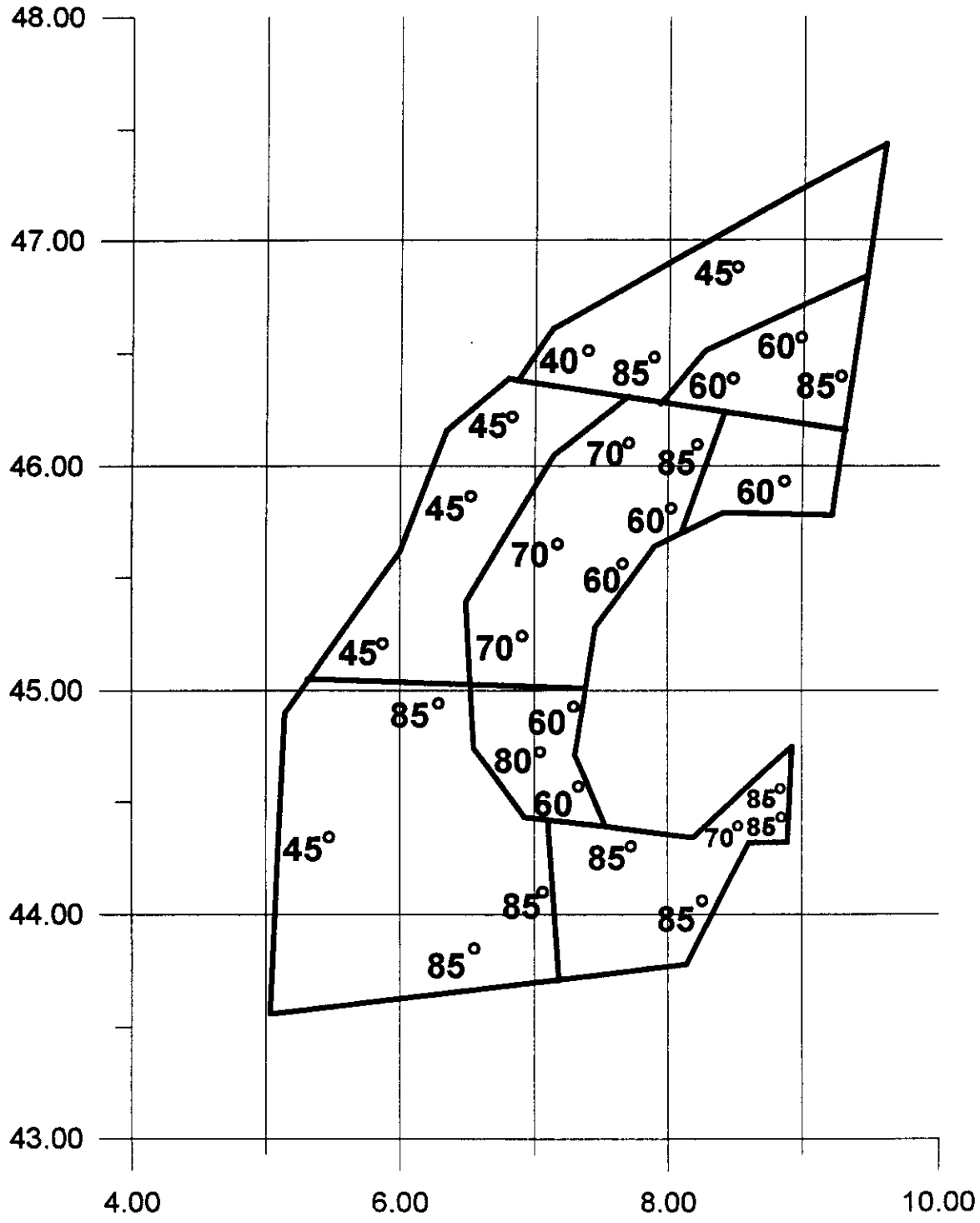

FIGURE 18 Block structure approximating the rough map of morphostructural zoning for Western Alps, the dip angles of fault zones are given.

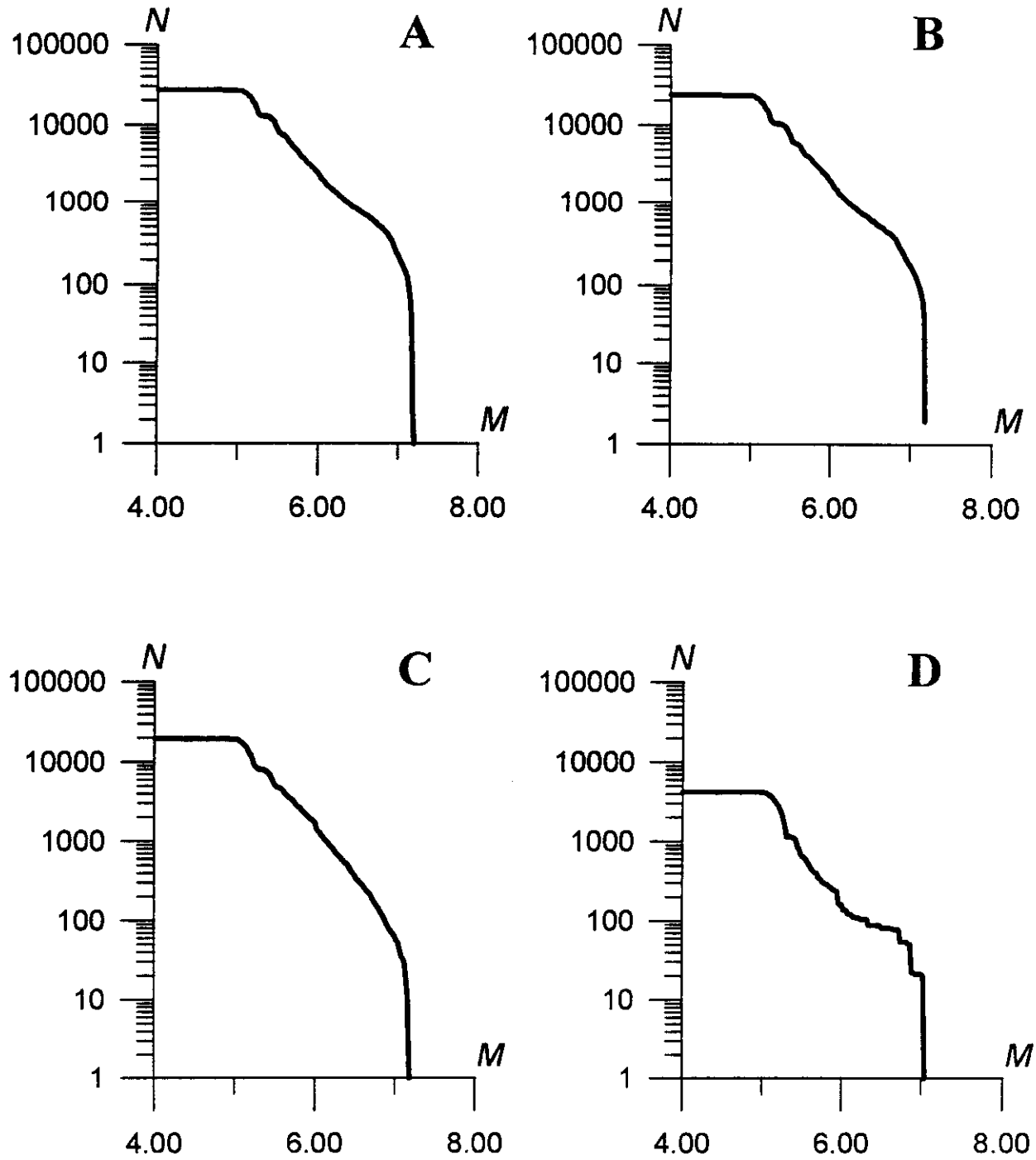

FIGURE 19 Accumulated frequency-magnitude plots for synthetic catalogs obtained with varying values of the angle between the vector of the boundary movement velocity and the north-oriented meridian: 30° (A), 45° (B), 60° (C), 90° (D).

The spatial distribution of epicenters in the synthetic earthquake catalog also depends on the direction of the boundary movement velocity vector. This is illustrated by Figure 20. One can therefore hope to obtain in the model a spatial distribution of epicenters close to that observed in the Western Alps by specifying a suitable movement of the boundaries and the underlying medium.

Dependence of the synthetic earthquake catalog on space discretization

As mentioned above, the space discretization was with ε = 7.5 km for the block model approximating the structure of the Vrancea region (V-model) and with ε = 5 km for that approximating the rough scheme of morphostructural zoning for the Western Alps (WS-model). Numerical simulation was carried out for these structures with different values of ε (for the latter structure, the variant with an angle of 45° between the velocity vector of boundary movement and the north was alone examined). The accumulated frequency-magnitude plots for the synthetic earthquake catalogs obtained are shown in Figure 21.

The values of ε equal to 5 km and 2.5 km were considered for the V-model, in addition to ε = 7.5 km. The frequency-magnitude plots (Fig. 21A) show that the magnitude range of the synthetic catalog involves increasingly smaller magnitudes, as ε decreases. At the same time the number of earthquakes in the magnitude range corresponding to the previous value of ε decreases. The slope (*b*-value) of the frequency-magnitude plot is changing as ε decreases. Note that for all values of ε considered there are abnormally large numbers of the largest events, to be interpreted as the presence of a "characteristic earthquake". The most pronounced effect is for the ε = 2.5 km curve. The total number of events in the synthetic earthquake catalogs obtained with different values of ε along with the minimum and maximum magnitudes are given in Table 8.

The values ε = 2.5 and 1 km were considered for the WS-model, in addition to ε = 5 km. The frequency-magnitude plots (Fig. 21B) show that, in contrast to the V-model, the decrease of ε has nearly no effect of decreasing the number of earthquakes in the magnitude range corresponding to the previous value of ε. The total number of earthquakes in the catalog increases due to extension of the magnitude range to smaller

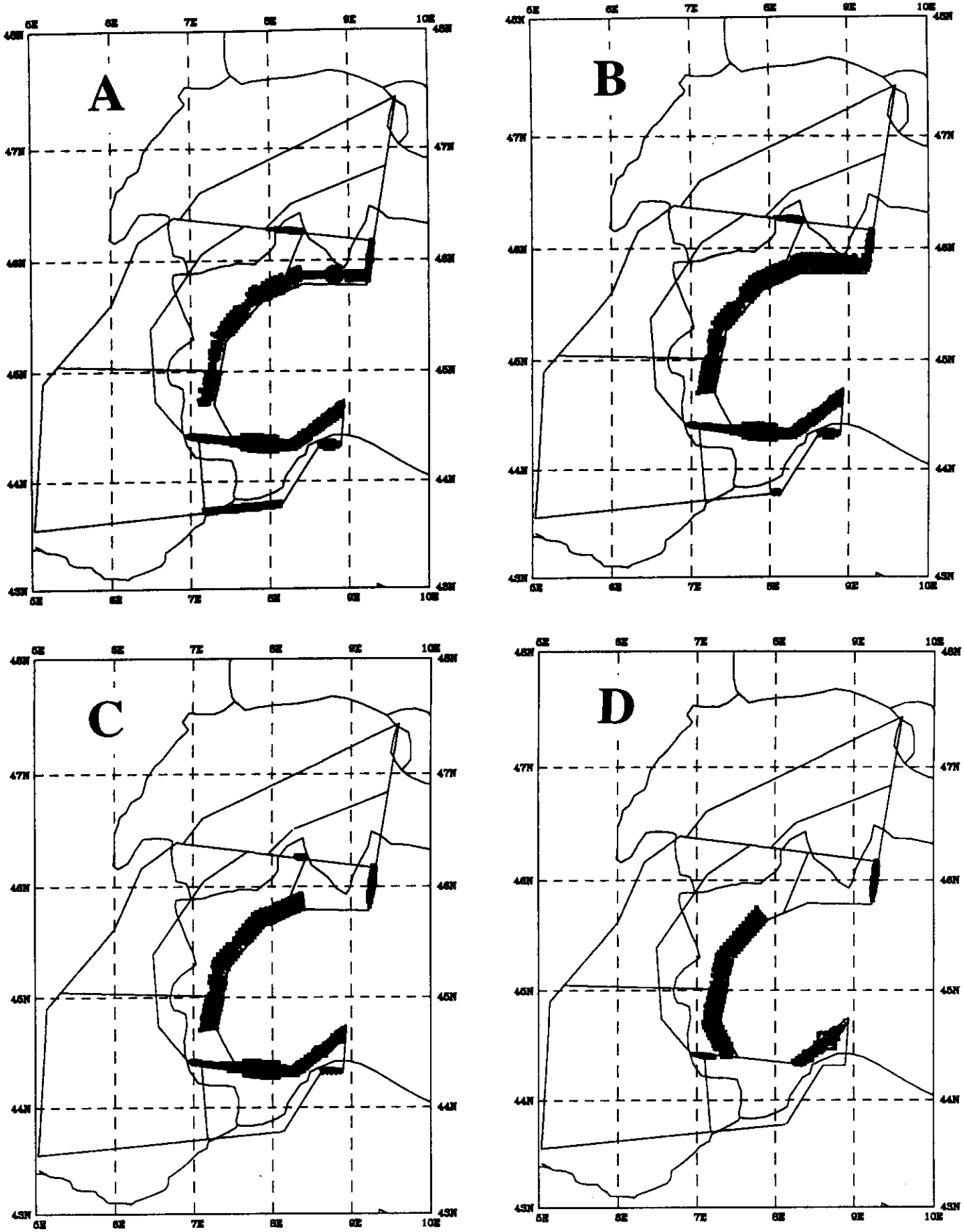

FIGURE 20 Maps of synthetic seismicity obtained in a block model approximating the rough map of morphostructural zoning for the Western Alps with varying values of the angle between the velocity vector of the boundary movement and the north-oriented meridian: A - 30°, B - 45°, C - 60°, D - 90°.

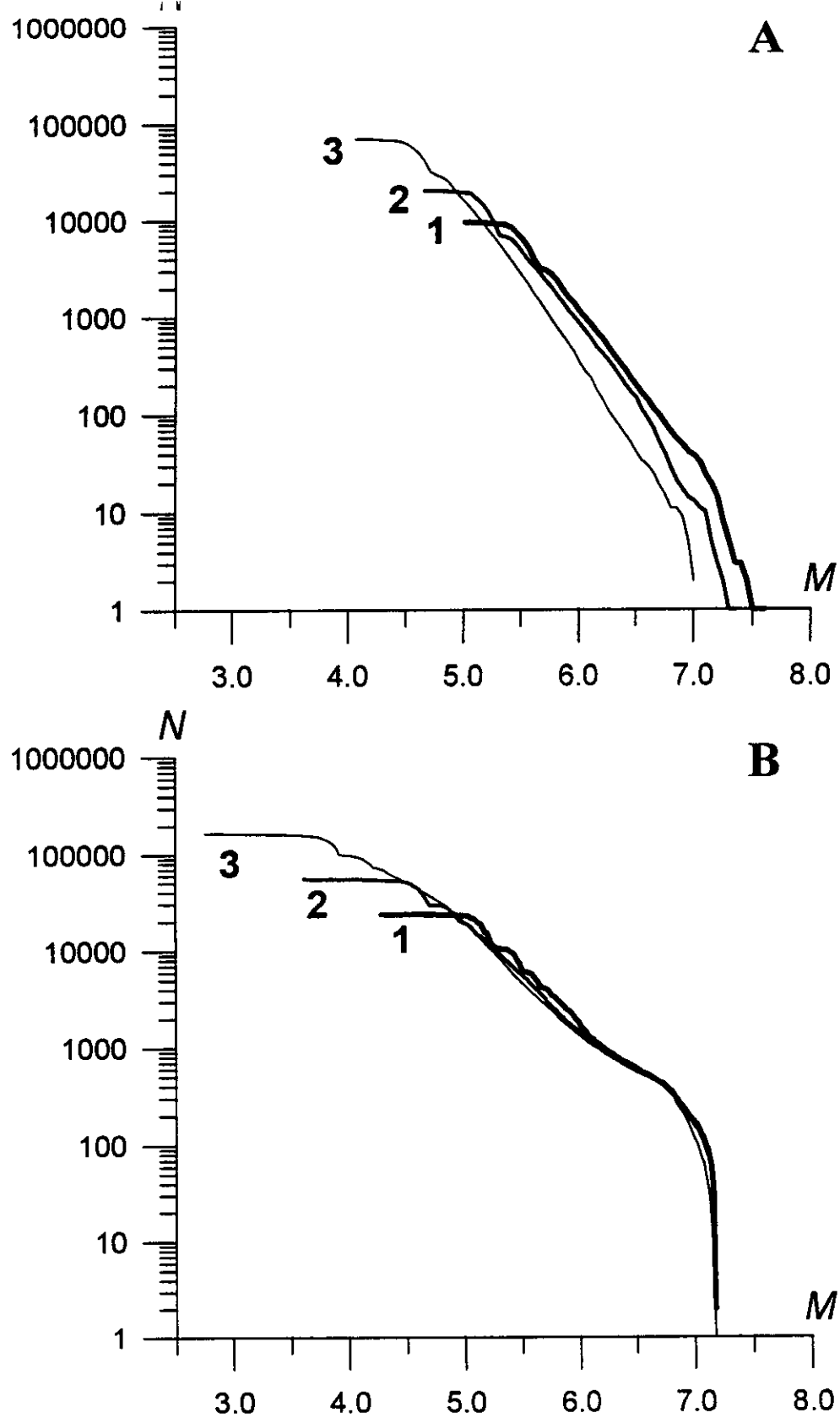

FIGURE 21 Accumulated frequency-magnitude plots for the synthetic catalogs obtained with different space discretization: A - structure approximating the Vrancea region (1 - 7.5 km, 2 - 5 km, 3 - 2.5 km); B - structure approximating the Western Alps (1 - 5 km, 2 - 2.5 km, 3 - 1 km).

TABLE 8 Dependence of characteristics of synthetic seismicity on the space discretization

Value of ε, km	Number of events in synthetic earthquake catalog	M_{min}	M_{max}
The model approximating the structure of Vrancea region			
7.5	9470	5.05	7.60
5	20197	4.70	7.35
2.5	70246	4.10	7.00
The model approximating the rough scheme of morphostructural zoning for Western Alps			
5	23630	4.30	7.20
2.5	55416	3.65	7.15
1	165770	2.80	7.20

magnitudes. The *b*-value does not change as ε decreases. Table 8 contains the total number of events in the catalogs and their minimum and maximum magnitudes for the WS-model.

It follows from (14) of GS that the minimum magnitude in the synthetic catalog must be about 3.9, 4.7, 5.3, and 5.6 for the values ε = 1, 2.5, 5, and 7.5 km, respectively. These minimum magnitudes are reflected in the behaviour of the curves in Figure 21. The values given in Table 8 are smaller, because they are controlled by a few number of the smallest cells resulting from discretization.

The results of these experiments in varying ε show that the sensitivity of a block model to space discretization depends on block structure geometry and the movements prescribed. It follows from Figure 21 that a synthetic earthquake catalog for which the linear part of the frequency-magnitude plot spans as much as 3 magnitude units can be obtained in a block model.

REFERENCES

Allegre,C.J., J.-L.Le Mouel, H.D.Chau, and C.Narteau (1995). Scaling organization of fracture tectonics (SOFT) and earthquake mechanism. Phys. Earth. Planet. Inter., **92**: 215-233.

Alekseevskaya,M.A., A.M.Gabrielov, A.D.Gvishiani, I.M.Gelfand, and E.Ya.Ranzman (1977). Formal morphostructural zoning of mountain territories. J. Geophys., *43*, 227-233.

Arinei,St. (1974). The Romanian Territory and Plate Tectonics, Technical Publishing House, Bucharest (in Romanian).

Bariere,B., and D.L.Turcotte (1994). Seismicity and self-organized criticality. Phys. Rev. E, **49**, *2*: 1151-1160.

Cisternas,A., P.Godefroy, A.Gvishiani, A.I.Gorshkov, V.Kosobokov, M.Lambert, E.Ranzman, J.Sallantin, H.Saldano, A.Soloviev, and C.Weber (1985). A dual approach to recognition of earthquake prone areas in the western Alps. Annales Geophysicae, **3**, *2*:249-270.

Dziewonski,A.M., and A.G.Prozorov (1984). Self-similar definition of clustering of earthquakes. In: Mathematical modeling and interpretation of geophysical data. Moscow: Nauka: 10-21 (Comput. Seismol.; Iss.16, in Russian).

Gabrielov,A.M., T.A.Levshina, and I.M.Rotwain (1990). Block model of earthquake sequence. Phys. Earth and Planet. Inter., **61**, 18-28.

Gabrielov,A., V.Kossobokov, and A.Soloviev (1994). Numerical simulation of block structure dynamics. In: Seismicity and Related Processes in the Environment, Vol.1. M.: Research and Coordinating Centre for Seismology and Engineering: 22-32.

Gabrielov,A., and A.Soloviev. Modelling of Block Structure Dynamics (1997). Fourth Workshop on Non-Linear Dynamics and Earthquake Prediction, 6 - 24 October 1997, Trieste: ICTP, 19 pp.

Gasilov,V., V.Maksimov, V.Kossobokov, A.Prozorov, and A.Soloviev (1995). Numerical Simulation of Block Structure Dynamics. II. Examples. Third Workshop on Non-Linear Dynamics and Earthquake Prediction, 6 - 17 November 1995, Trieste: ICTP, H4.SMR/879-3, 48 pp.

Global Hypocenters Data Base CD-ROM (1994). Denver CO, NEIC/USGS.

Gorshkov,A.I. and A.A.Soloviev (1996). The Western Alps: Numerical modelling of block structure and seismicity. In: XXV General Assembly of the European Seismological Commission, September 9-14, 1996, Reykjavik, Iceland. Abstracts, 66.

Gutenberg,B., and C.F.Richter (1956). Earthquake magnitude, intensity, energy and acceleration, Bull. Seism. Soc. Am., **46**: 105-145.

Hattori,S. (1974). Regional distribution of b-value in the world. Bull. Intern. Inst. Seismol. and Earth Eng., **12**: 39-58.

Kagan,Y. and L.Knopoff (1978). Statistical study of the occurrence of shallow earthquakes. Geophys. J. R. Astron. Soc., **55**: 67-86.

Keilis-Borok,V.I., L.Knopoff, and I.M.Rotwain (1980) Bursts of aftershocks, long-term precursors of strong earthquakes. Nature, **283**: 258-263.

Keilis-Borok,V.I., I.M.Rotwain, and A.A.Soloviev (1997). Numerical modeling of block structure dynamics: dependence of a synthetic earthquake flow on the structure separateness and boundary movements. Journal of Seismology (in press).

Kronrod,T.L. (1984). Seismicity parameters of the main regions of the high seismic activity. In: Keilis-Borok,V.I., and A.L.Levshin (eds). Logical and Computational Methods in Seismology. Moscow: Nauka: 36-57 (Comput. Seismol.; Iss.17, in Russian).

Maksimov,V.I. and A.A.Soloviev (1996). Clustering of earthquakes in block model of lithosphere dynamics. In: Keilis-Borok,V.I., and A.L.Molchan (eds). Modern problems of seismicity and Earth dynamics. Moscow: Nauka: 148-152 (Comput. Seismol.; Iss. 28, in Russian).

McKenzie,D.P. (1970). Plate tectonics of the Mediterranean region. Nature, **226**: 239-243.

Mogi,K. (1962). Magnitude-frequency relation for elastic shocks accompanying fractures of various materials and some related problems in earthquakes. Bull. Earthq. Inst. Tokyo Univ., **40**: 831-853.

Mocanu,V.I. (1993). Final report "Go West" Programme. Proposal No: 4609. Contract No: CIPA3510PL924609. Subject: "Methods for Investigation of Different Kinds of Lithospheric Plates in Europe". Period September-December 1993 (Scientific Supervisor: Prof.G.F.Panza).

Molchan,G.M. and O.E.Dmitrieva (1991). Identification of aftershocks: methods and new approach. In: Modern methods for seismic data processing. Moscow: Nauka: 19-50 (Comput. Seismol.; Iss.24, in Russian).

Moldoveanu,C.L., O.V.Novicova, I.A.Vorobieva, and M.Popa (1995) The updated Vrancea seismoactive region catalog. ICTP, Internal report, IC/95/104.

Newman,W.I., D.L.Turcotte, and A.M.Gabrielov (1995). Log-periodic behaviour of a hierarchical failure model with application to precursory seismic activation. Phys. Rev. E., **52**: 4827-4835.

Novikova,O.V., I.A.Vorobieva, D.Enescu, M.Radulian, I.Kuznetzov, and G.Panza (1995). Prediction of Strong Earthquakes in Vrancea, Romania, Using the CN Algorithm. PAGEOPH, **145**, 277-296.

Panza,G.F., A.A.Soloviev, and I.A.Vorobieva (1997). Numerical Modelling of Block-Structure Dynamics: Application to the Vrancea Region. PAGEOPH, **149**: 313-336.

Radu,C.(1979). Catalogue of strong earthquakes originated on the Romanian territory, Part II: 1901-1979. In: Seismological Research on the Earthquake of March 4, 1977 - Monograph (eds. I.Cornea and C.Radu, Central Institute of Physics, Bucharest)

Shamina,O.G., V.A.Budnikov, S.D.Vinogradov et al. (1980). Laboratory experiments on the Physics of the earthquake source. In: Physical Processes in Earthquake Sources. Moscow: Nauka: 56-68 (in Russian).

Shaw,B.E., J.M.Carlson, and J.S.Langer (1992). Patterns of seismic activity preceding large earthquakes. J. Geophys. Res., **97**: 479.

Sherman,S.I., S.A.Borniakov, and V.Yu.Buddo (1983). Areas of Dynamic Effects of Faults. Novosibirsk: Nauka: 111 pp. (in Russian).

Sobolev,P.O., A.A.Soloviev, and I.M.Rotwain (1996). Modelling of lithosphere dynamics and seismicity for the Near East region. In: Keilis-Borok,V.I., and G.M.Molchan (eds). Modern Problems of Seismicity and Earth Dynamics. Moscow: Nauka: 131-147 (Comput. Seismol.; Iss.28, in Russian).

Soloviev,A.A. (1995). Modeling of block structure dynamics and seismicity. In: European Seismological Commission, XXIV General Assembly, 1994 September 19-24, Athens, Greece, Proceedings and Activity Report 1992-1994, Vol.III: University

of Athens, Faculty of Sciences, Subfaculty of Geosciences, Department of Geophysics & Geothermy: 1258-1267.

Turcotte,D.L. (1992) Fractals and Chaos in Geophysics. Cambridge: Cambridge University Press.

Utsu,T. and A.Seki (1954). A relation between the area of aftershock region and the energy of main shock. J. Seism. Soc. Japan, 7, 233-240.

Vorobieva,I.A. and A.A.Soloviev (1997). Connection between space distribution of earthquake epicenters and movement of lithosphere blocks. Doklady of Russian Ac. Sci. (in Russian, in press).